Tectonics

RESEARCH ARTICLE
10.1029/2019TC005927

Structural Evolution at the Northeast North German Basin Margin: From Initial Triassic Salt Movement to Late Cretaceous-Cenozoic Remobilization

Niklas Ahlrichs[1,2], Christian Hübscher[2], Vera Noack[1], Michael Schnabel[3], Volkmar Damm[3], and Charlotte M. Krawczyk[4,5]

[1]Federal Institute for Geosciences and Natural Resources (BGR), Berlin Branch Office, Berlin, Germany, [2]Institute of Geophysics, Center for Earth System Research and Sustainability, Universität Hamburg, Hamburg, Germany, [3]Federal Institute for Geosciences and Natural Resources (BGR), Geozentrum Hannover, Hannover, Germany, [4]Institute for Applied Geosciences, Technical University Berlin, Berlin, Germany, [5]GFZ German Research Centre for Geosciences, Potsdam, Germany

Key Points:
- A regional high-resolution seismic profile continuously images the SW Baltic Sea subsurface from the Zechstein salt base to the seafloor
- Late Triassic salt movement and Late Cretaceous-Cenozoic remobilization correlate with regional tectonics at the North German Basin margin
- The tectonic evolution of salt pillows is discussed in terms of thin-skinned extensional/compressional deformation and gravity gliding

Correspondence to:
N. Ahlrichs,
niklas.ahlrichs@bgr.de

Citation:
Ahlrichs, N., Hübscher, C., Noack, V., Schnabel, M., Damm, V., & Krawczyk, C. M. (2020). Structural evolution at the northeast North German Basin margin: From initial Triassic salt movement to Late Cretaceous-Cenozoic remobilization. *Tectonics*, *39*, e2019TC005927. https://doi.org/10.1029/2019TC005927

Received 11 OCT 2019
Accepted 5 JUN 2020
Accepted article online 12 JUN 2020

Abstract In this study, we investigate the regional tectonic impact on salt movement at the northeastern margin of the intracontinental North German Basin. We discuss the evolution of salt pillows in the Bay of Mecklenburg in the light of thick- and thin-skinned tectonics, including gravity gliding, and differential loading using seismic imaging. Stratigraphic and structural interpretation of a 170 km long, multichannel seismic line, extending from the Bay of Mecklenburg to northeast of Rügen Island, incorporates well information of nearby onshore wells. This new high-resolution seismic line completely images the stratigraphic and tectonic pattern of the subsurface, from the base of the Zechstein to the seafloor. Our analysis reveals that subsidence during Late Triassic to Early Cretaceous at the northeastern basin margin was associated with transtensional dextral strike slip movement within the Trans-European Suture Zone. We reinterpret the Werre and Prerow Fault Zones west of Rügen Island as an inverted, thin-skinned normal fault system associated with the formation of the Western Pomeranian Fault System. Salt movement in the Bay of Mecklenburg was initiated in the Late Triassic and lasted until the Early Jurassic. A second phase of salt pillow growth occurred during the Coniacian until Cenozoic and correlates with compression-related regional basin inversion due to the onset of the Africa-Iberia-Europe convergence. Thin-skinned extensional initialization of salt pillow growth and compressional salt remobilization explains salt pillow evolution in the Bay of Mecklenburg. Additionally, we discuss an impact of gravity gliding on salt pillow evolution induced by basin margin tilt.

1. Introduction

Salt structures within continental basins frequently form as a result of plate and intraplate tectonic deformation, often in the vicinity of prominent basement faults due to extension or shortening (Callot et al., 2012; Coleman et al., 2017; Krzywiec et al., 2019; Pichel et al., 2019; Scheck-Wenderoth et al., 2008; Vejbaek, 1997; Warren, 2008; Warsitzka et al., 2018). In the presence of a salt layer that effectively decouples the overburden from the underlying basement faulting, thin-skinned deformation can alternatively initiate the development of salt structures. Differential sediment load is another important reason for the formation of salt structures (e.g., Blanc et al., 2003; Callot et al., 2012; Davis & Engelder, 1985; Hudec & Jackson, 2007; Jackson & Hudec, 2017; Jaritz, 1973; Kockel, 1999; Kukla et al., 2008; Stewart, 2007; Trusheim, 1960; Vendeville & Jackson, 1992; Warsitzka et al., 2018). Salt tectonics at continental margins has been intensively studied because of the availability of high-quality continuous seismic images from the basement up to the seafloor. Here along the passive margins, widely present gravity-driven deformation by means of gravity gliding and gravity spreading dominates the scientific discussion about the principle salt tectonic mechanisms. Gravity gliding refers to downdip gliding of the salt-sediment package caused by basin margin tilt, whereas gravity spreading is driven by differential sediment load (Brun & Fort, 2011, 2012; Cobbold & Szatmari, 1991; Jackson & Hudec, 2005; Rowan et al., 2004, 2012). The effect of gravity-driven salt flow in the Southern Permian Basin has been rarely studied and often remained speculative (overview by Warsitzka et al., 2018. Allertal: Best, 1996; North Sea: Steward & Coward, 1996; Thieme & Rockenbauch, 2001; Ems Trough: Mohr et al., 2005; Rheinsberg Trough: Scheck et al., 2003; Polish Basin: Krzywiec, 2012).

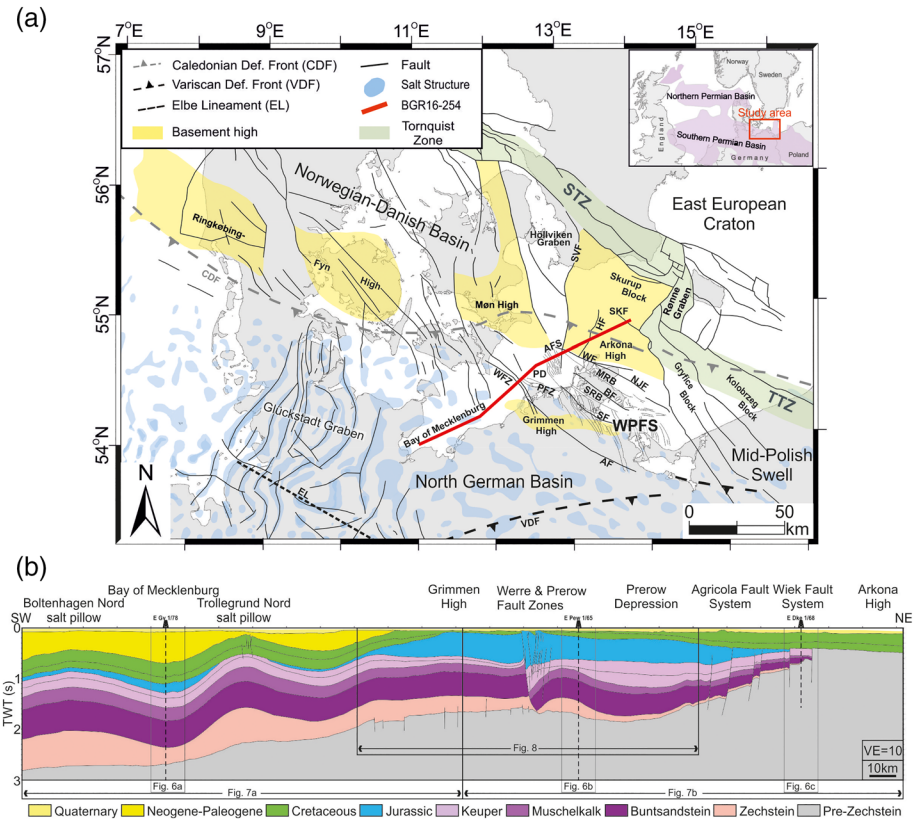

Figure 1. (a) Tectonic map of the North German Basin including major geological structures (based on Vejbaek & Britze, 1994; Schlüter et al., 1997; Baldschuhn et al., 2001; Pharaoh et al., 2010; Al Hseinat & Hübscher, 2017; Seidel et al., 2018; Mazur et al., 2020). Inset shows approximate outline of the northern and southern Permian Basin. Red line marks position of profile BGR16-254 analyzed in this study. AF = Anklam Fault; AFS = Agricola Fault System; BF = Bergen Fault; CDF = Caledonian Deformation Front; EL = Elbe Lineament; HF = Hiddensee Fault; MRB = Middle Rügen Block; NJF = Nord Jasmund Fault; PD = Prerow Depression; PFZ = Prerow Fault Zone; SF = Strelasund Fault; SKF = Skurup Fault; SRB = South Rügen Block; STZ = Sorgenfrei-Tornquist Zone; SVF = Svedala Fault; TTZ = Tornquist-Teisseyre Zone; VDF = Variscan Deformation Front; WFZ = Werre Fault Zone; WF = Wiek Fault; WPFS = Western Pomeranian Fault System. (b) Condensed geological cross section along profile BGR16-254 analyzed in this study, showing main structures and stratigraphic features. Seismic data acquired during cruise MSM52 (Hübscher et al., 2016).

Therefore, a detailed analysis of gravity-driven deformation and its contribution to the salt tectonic evolution in intracontinental basins remains an open task. The Baltic Sea sector of the North German Basin (NGB) marks an excellent study area to further investigate the impact of regional tectonics on salt mobilization. The major structural element bounding the study area in the east is the Tornquist Zone. It consists of two segments, the southern Tornquist-Teisseyre Zone (TTZ) and the northern Sorgenfrei-Tornquist Zone (STZ). The latter represents the southwestern border between the stable Precambrian East European Craton (EEC) and its southwestern intensively faulted part (Erlström et al., 1997; Eugeno, 1988). The TTZ separates the EEC from the Paleozoic crust of Central Europe (Berthelsen, 1992). However, recent studies by Mazur et al. (2015) support the suggestion of Berthelsen (1998) that the TTZ represents a pseudo-suture and therefore can be regarded as an intraplate feature of the EEC. Adjacent to the TTZ, the Permian-Mesozoic Polish Basin developed contemporaneously to the NGB. Both are parts of the Southern Permian Basin, which is included in the Central European Basin System, a series of related intracontinental basins spreading from Britain to the Polish mainland (Maystrenko et al., 2008; Pharaoh et al., 2010). Within the central part of the NGB, the prominent Mesozoic-Cenozoic Glückstadt Graben marks the western border of the study area (Figure 1).

The structural style of post-Permian deposits in the NGB is strongly influenced by salt tectonics resulting in many salt structures consisting of Upper Permian Zechstein evaporites. Several past marine geophysical studies, such as EUGENO (1988), BABEL Working Group (1991, 1993), Petrobaltic (e.g., Rempel, 1992), SASO (Schlüter et al., 1997), and DEKORP-BASIN (1999) documented major tectonic events in the Baltic Sea sector of the NGB. These projects focused mainly on a better understanding of deep-crustal structures. Studies carried out within the Neobaltic project (Al Hseinat et al., 2016; Al Hseinat & Hübscher, 2017; Hansen et al., 2005, 2007; Hübscher et al., 2004, 2010) and studies by Kossow et al. (2000), Krawczyk et al. (2002), Kossow and Krawczyk (2002), Maystrenko et al. (2005, 2012), Seidel et al. (2018), and Deutschmann et al. (2018) provided further insight into Mesozoic and Cenozoic tectonics. These authors discussed the salt tectonic evolution in the context of its regional tectonic framework. However, they did not further elaborate on the causative processes due to data gaps along the basin margin and incomplete seismic imaging from the base of the Zechstein to the seafloor.

This study is part of the "StrucFlow" project, where we investigate the kinematic history of the northeast NGB margin from initial Triassic salt movement to Cretaceous-Cenozoic basin inversion and salt remobilization by means of new high-resolution reflection seismic data. This data set closes the gap between former surveys and studies in terms of both seismic resolution and depth penetration in the study area. This allows a first-time comprehensive analysis of emplacement and timing of salt movement from deposition to present day in the offshore sector of the NGB. We start our studies by stratigraphic interpretation, fault interpretation, and analysis of local depocenters along a 170 km-long seismic profile in order to identify and date salt movements. The profile images a significant part of the northeast NGB covering the deeper basin and its transistion to the basin margin. We discuss the impact of regional tectonics on salt movement at the northeast NGB margin in the light of thin- and thick-skinned tectonics, differential loading, and an impact of gravity-induced salt flow. This study provides new insight into the interaction between reactivated deep-seated fault zones and salt movement caused by regional tectonic stress. Our findings add to the understanding of the complex structural evolution of salt-floored intracontinental basins in their marginal domain.

2. Geological Setting

2.1. Regional Geological Setting of the NGB

The NGB is part of the Southern Permian Basin, which extends from Britain over central Europe to Poland (e.g., Maystrenko et al., 2008) (inset of Figure 1). The basin is an intracontinental basin with a complex structural development from the Carboniferous to present. Its evolution began with WNW-ESE extension and transtension in the latest Carboniferous-Permian accompanied by the deposition of Carboniferous volcanics, coal, and Lower Permian volcanics and clastics (Bachmann et al., 2008; Maystrenko et al., 2008; Ziegler, 1990). Several marine transgressions at paleogeographic low latitudes led to extensive evaporation and the deposition of the Permian Zechstein (Wuchiapingian-Changshingian) evaporites. These evaporites formed numerous salt structures during the Mesozoic-Cenozoic (Bachmann et al., 2010; Maystrenko et al., 2008; Strohmenger et al., 1996; Tucker, 1991; Warsitzka et al., 2018). Thermal subsidence and phases of E-W extension characterize the Triassic basin evolution (Maystrenko et al., 2008; van Wees et al., 2000; Ziegler, 1990). From Middle Jurassic to Late Jurassic, thermal doming in the North Sea (centered in the Central Graben) caused large-scale uplift and erosion of Jurassic and partly Triassic deposits in the NGB (Graversen, 2006; Underhill, 1998). In Late Cretaceous times, NW-SE to N-S directed shortening changed the overall stress regime to compressive. Compressional stress caused inversion of normal faults, the initiation of reverse faults and folding. This compressive event marks the onset of the Africa-Iberia-Europe convergence. Additional pulses of uplift and inversion followed in the Early Paleocene and Late Eocene, accompanied by the development of E-W to NW-SE oriented extension (Bachmann et al., 2010; Kley, 2018; Kley & Voigt, 2008; Maystrenko et al., 2008).

2.2. The Northeast NGB Margin

Major structural elements bounding the NGB are the Ringkøbing-Fyn, Møn, and Arkona Highs in the north and the Mid-Polish Swell (MPS) in the east (Figure 1). The study area covers the region from the eastern Glückstadt Graben in the west toward the MPS (Figure 1). This area includes deeper parts as well as the northeastern margin of the NGB. The northeastern basin margin developed partly above the transition of

the Paleozoic lithosphere of central Europe to the Precambrian EEC. The crustal border marking this transition consists of a complex assemblage of terranes. This zone is termed the Trans-European Suture Zone, which spans between the Caledonian Deformation Front in the north and the Elbe Line in the south (Berthelsen, 1992; Guterch et al., 2010; Pharaoh, 1999, and references therein) (Figure 1). The area around Rügen Island is characterized by the Western Pomeranian Fault System, a set of smaller fault zones (e.g., Werre Fault Zone [WFZ], Prerow Fault Zone, and Agricola Fault System [AFS]; see Figure 1 for location), whose development is associated with the Trans-European Suture Zone (Krauss & Mayer, 2004). The crust within this area consists of Caledonian and Variscan consolidated terranes (Berthelsen, 1992; Brink et al., 1990; Krawczyk et al., 2008a, 2008b; Maystrenko et al., 2008; Ziegler, 1990). Formation of the NGB began in the Late Paleozoic and was associated with extensive volcanism, faulting, lithospheric thinning, and following thermal relaxation of the thinned lithosphere (Benek et al., 1996; Gast et al., 1998; Scheck et al., 1999; van Wees et al., 2000; Ziegler, 1990). The main phase of thermal subsidence started in the Early Permian and lasted until Middle Triassic times (Kossow et al., 2000; van Wees et al., 2000). The lowermost basin fill at the northeast basin margin consists of upper Carboniferous to Permian volcanics overlain by lower Permian sediments (Geißler et al., 2008; Scheck & Bayer, 1999) (Figure 2). Several marine transgressions of the epicontinental Zechstein Sea in combination with repeatedly restricted seawater influx under arid climate conditions led to the deposition of the Zechstein evaporites. The Zechstein succession involves seven cyclic units (cyclothems) each consisting of clay/carbonates, anhydrite, and halite sequences (Strohmenger et al., 1996; Tucker, 1991). However, only five major cyclothems are present in the study area. The Werra (Z1) cyclothem consists mostly of anhydrite, which is less mobile than halite due to its higher viscosity. The Stassfurt (Z2), Leine (Z3), Aller (Z4), and Ohre (Z5) cyclothems contain thicker layers of mobile halite and less-dominant anhydrite layers. A thicker anhydrite rich layer developed in the Leine cyclothem (e.g., Katzung, 2004; Kossow et al., 2000; Warren, 2008). The Stassfurt (Z2) sequence represents the most important cyclothem for salt tectonics in the study area due to its thick halite sequence (Kossow et al., 2000; Warren, 2008). Thickness of the Zechstein succession decreases toward the northeast NGB margin (Figure 3). Mobile halite segments gradually reduce and pinch out northeast of the Prerow Fault Zone (Figures 1 and 3). Near the west of Rügen Island, halite and anhydrite are absent within the Zechstein. Here, carbonates and siltstones, mostly of the Stassfurt cyclothem, dominate the marginal Zechstein succession (Figure 3) (Kaiser, 2001; Zagora & Zagora, 1997).

The overlaying Triassic Buntsandstein succession consists mostly of intercalated claystone and siltstone deposited during accelerated basin subsidence (Hoth et al., 1993; Kossow & Krawczyk, 2002; van Wees et al., 2000). A regional rise in sea level in the Middle Triassic led to the deposition of the Muschelkalk platform carbonates. Major faulting and indications for halokinesis are absent in the study area within the Buntsandstein and Muschelkalk units (Kossow & Krawczyk, 2002).

A eustatic sea level drop established terrestrial conditions in the Triassic Keuper (Nöldeke & Schwab, 1976; Scheck & Bayer, 1999). E-W directed extension occurred in the Glückstadt Graben resulting in salt movement in the surrounding area (Frisch & Kockel, 1999; Jaritz, 1987; Maystrenko et al., 2006). A major erosional event occurred within the Keuper. Beutler and Schüler (1978) described the event as the "Altkimmerische Hauptdiskordanz" (Early Cimmerian Unconformity [ECU] in Bachmann et al., 2010). Erosion of the entire Lower Keuper down to Muschelkalk deposits occurred at the basin margin in the western Rügen area. Toward the basin center, Lower Keuper deposits are preserved (Figure 4). This erosional event was contemporaneous to the development of the NE-SW trending Western Pomeranian Fault System between the Wiek and Anklam faults (Beutler et al., 2012; Frisch & Kockel, 1999; Kossow et al., 2000; Seidel et al., 2018) (Figure 1). The fault system consists of several fault zones and smaller fault systems bordering Y-shaped graben structures such as the Werre and Prerow Fault Zones and AFS. Their formation is associated with dextral transtensional movements above the Trans-European Suture Zone during the Late Triassic to Early Cretaceous (Deutschmann et al., 2018; Krauss & Mayer, 2004; Seidel et al., 2018). The authors attribute this Mesozoic dextral shear stress with NE-SW extension to the reactivation of existing NW-SE oriented Paleozoic faults, which were decoupled from the supra-salt succession by the partly overlying Zechstein salt.

A major transgression in the Rhaetian led to renewed sedimentation in shallow marine conditions lasting throughout the Jurassic (Kossow et al., 2000). From Late Jurassic times until the Albian, subsidence was interrupted by a period of uplift and nondeposition at the northeastern basin margin. Erosion of almost

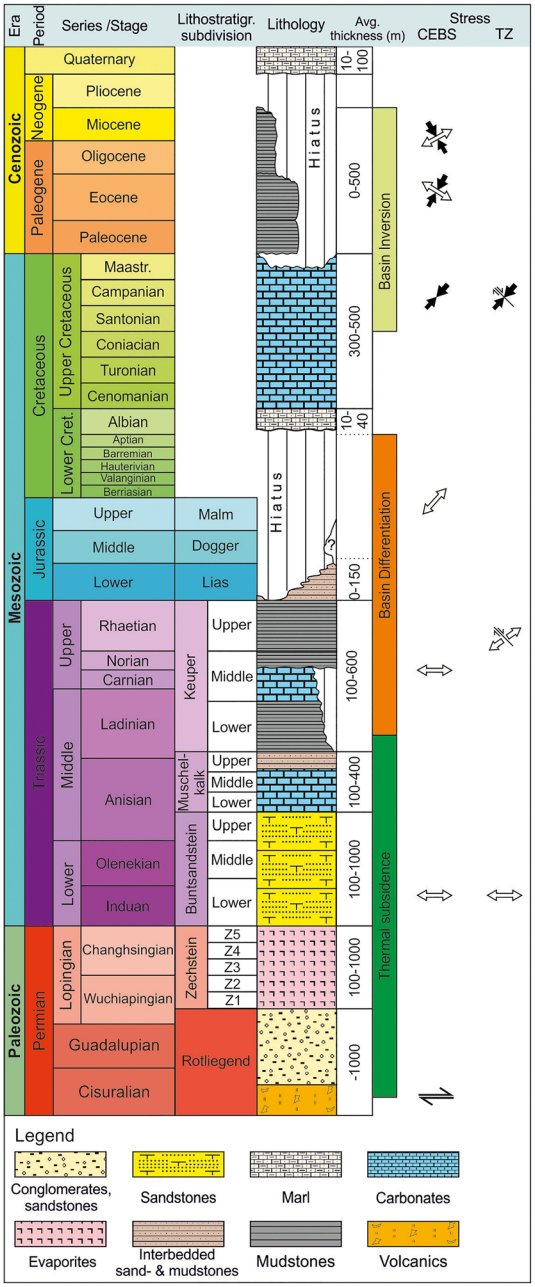

Figure 2. Lithostratigraphic chart showing the dominant lithology and average thickness within the study area. Main phases of the development of the Central European Basin System are shown together with main stress direction. (based on Kossow & Krawczyk, 2002; Kley & Voigt, 2008; Kley & Voigt, 2008; Al Hseinat & Hübscher, 2017; Seidel et al., 2018. Average thickness is based upon Hoth et al., 1993).

the entire Jurassic sequence and in some areas even Keuper units occurred. Lower Jurassic sediments preserved in rim synclines indicate active salt movement during this time (Kossow et al., 2000; Maystrenko et al., 2005). Due to an observed increasing amount of erosion from the Bay of Mecklenburg in westward direction, Hübscher et al. (2010) and Al Hseinat and Hübscher (2017) associate the uplift with the Central North Sea doming event (Graversen, 2006; Underhill & Partington, 1993; Ziegler, 1990).

Rising sea levels during the Albian led to a major transgression and resumed sedimentation (Vejbaek et al., 2010). Shallow marine conditions and rising eustatic sea level prevailed until early Turonian times and mark a period of relative tectonic quiescence (Kossow & Krawczyk, 2002; Scheck & Bayer, 1999;

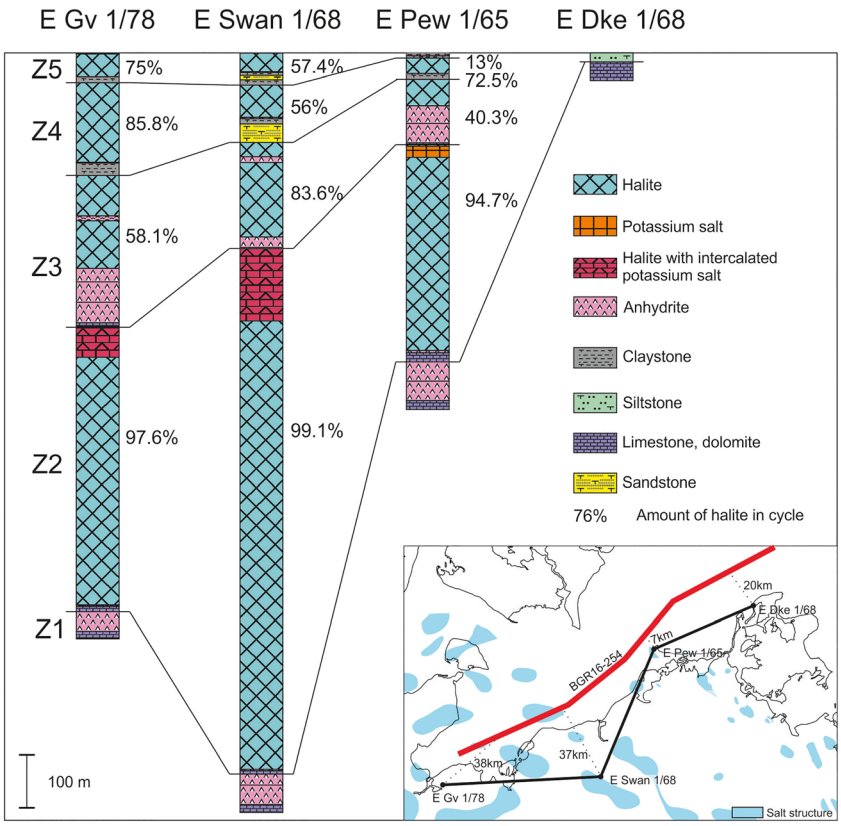

Figure 3. Correlation of Zechstein cyclothems along the northeast North German Basin margin. Z1 = Werra; Z2 = Stassfurt; Z3 = Leine; Z4 = Aller; Z5 = Ohre. Well information compiled after Hoth et al. (1993). Inset: salt structures after Reinhold et al. (2008). Numbers represent approximate distance from the well to similar position regarding salt distribution on the profile BGR16-254 (see also Figure 1 for location).

Vejbaek et al., 2010). Sea level remained high until the Campanian. From the Santonian until the Cenozoic, the study area underwent several pulses of uplift and inversion associated with major plate reorganization and the onset of the Africa-Iberia-Europe convergence and Pyrenees and Alpine orogenies (Kley, 2018; Kley & Voigt, 2008). Horizontal shortening induced during the Late Cretaceous (late Turonian/Santonian to Maastrichtian) inversion pulse reactivated preexisting basement faults leading to uplift and erosion at the northeastern basin margin (Kley, 2018; Kley & Voigt, 2008; Kossow & Krawczyk, 2002). Uplift of the Grimmen High resulted in complete erosion of the Cretaceous deposits so that Cenozoic successions directly overlay Lower Jurassic sediments along this WNW striking basin edge structure. The pinch out of mobile Zechstein salt northeast of the Grimmen High is interpreted to have increased the basal friction between decoupled overburden and the basement. This caused increased resistance against the northward propagating overburden deformation, which resulted in uplift of the Grimmen High (Kossow et al., 2000; Kossow & Krawczyk, 2002).

Further uplift events during the Cenozoic occurred during the Paleocene and late Eocene to late Oligocene. However, their exact timing and spatial extent are an aspect of recent discussion (Kley, 2018). Cenozoic sediments above salt pillows in the Bay of Mecklenburg reveal quite strong thickness reduction and increased salt pillow growth from Late Cretaceous to Cenozoic. A change of stress orientation from NE-SW to NW-SE directed extension during the Neogene caused another phase of intensified salt movement and fault reactivation (Al Hseinat & Hübscher, 2017; Hübscher et al., 2010; Kammann et al., 2016).

2.3. Salt Tectonic Framework of the Northeastern NGB Margin

According to several previous studies, many salt structures in the NGB were triggered and grew during multiple phases of extension. Salt structure growth is linked to normal faulting of the subsalt basement (e.g.,

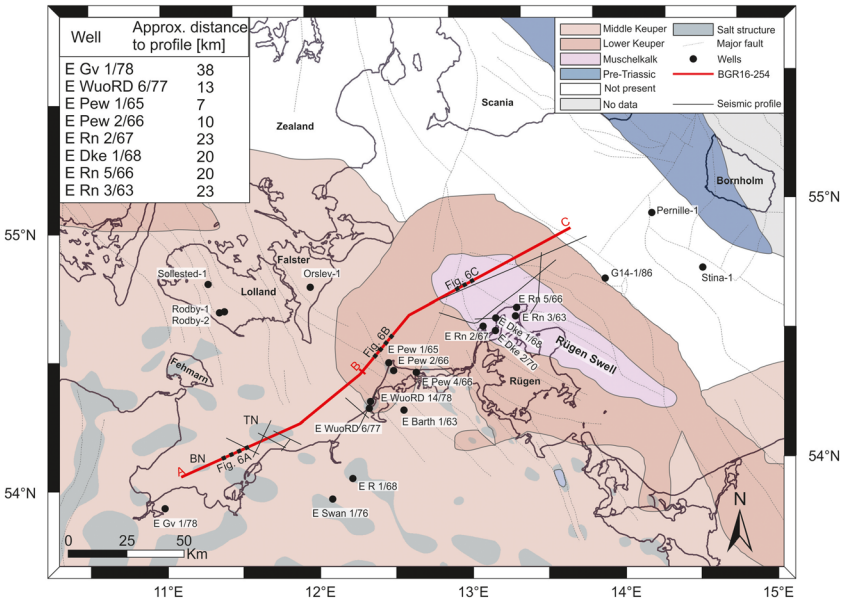

Figure 4. Subcrop map of the Early Cimmerian Unconformity (ECU) (Base Norian; German: "Altkimmerische Hauptdiskordanz," Beutler & Schüler, 1978) including onshore wells used for stratigraphic correlation. Table marks the approximate distance of most important wells to the interpreted profile. Note the trend of the ECU resting on Muschelkalk deposits near northern Rügen Island to Lower and Middle Keuper sediments toward the Bay of Mecklenburg. Compiled after Schlüter et al. (1997), Bachmann et al. (2010), Reinhold et al. (2008), and Al Hseinat and Hübscher (2017). TN = Trollegrund Nord salt pillow; BN = Boltenhagen Nord salt pillow. Dashed black segments on the seismic profile BGR16-254 (red line) are shown in Figure 6. Positions A-B and B-C mark segments of the seismic profile shown in Figures 7a and 7b, respectively.

structures within the Glückstadt Graben) (Jaritz, 1973; Kockel, 1999, 2002; Kukla et al., 2008; Maystrenko et al., 2005; Mohr et al., 2005; Warren, 2008). Salt structures in the northeastern part of the NGB have been widely studied with respect to their distribution, geometry, and timing. Salt movement was analyzed as a function of the regional tectonic framework in the context of early stage salt movement within a continental basin (Hübscher et al., 2010; Kossow et al., 2000; Kossow & Krawczyk, 2002; Scheck et al., 2003; Warsitzka et al., 2018; Zöllner et al., 2008). However, a direct link between salt structure distribution and basement faults was not found.

The development of salt pillows in the Bay of Mecklenburg began after the deposition of the Triassic Muschelkalk (Zöllner et al., 2008). Hübscher et al. (2010) showed a Late Triassic initiation of salt pillow growth caused by E-W extension. This was followed by a phase of (salt) tectonic quiescence from Early to latest Cretaceous times. A second phase of pronounced salt movements from the latest Cretaceous to Paleogene is related to basin inversion caused by compression (Kossow & Krawczyk, 2002). Crustal shortening induced basinwide tightening of preexisting anticlinal structures, which amplified salt pillows. However, the amount of shortening significantly decreases from south to north. Hence, the effect of shortening on salt structures close to the northeastern basin margin remains quite unclear. Al Hseinat and Hübscher (2017) identified three major fault trends affecting salt movement in the study area. The authors relate NNE-SSW and N-S trending faults to the development of the Glückstadt Graben and the NW-SE trending faults to movement at the Tornquist Zone (Figure 1).

3. Database and Methods

In March 2016, the University of Hamburg, in cooperation with the Federal Institute for Geosciences and Natural Resources (BGR), University of Greifswald, Polish Academy of Sciences, Uppsala University, and the German Research Centre for Geosciences Potsdam, acquired 3,500 km of high-resolution multichannel seismic data onboard RV Maria S. Merian, cruise MSM52, as part of the "BalTec" project (Hübscher et al., 2016). The seismic equipment consisted of an eight GI-Gun cluster (45/105 in^3) allowing for deep

(a)

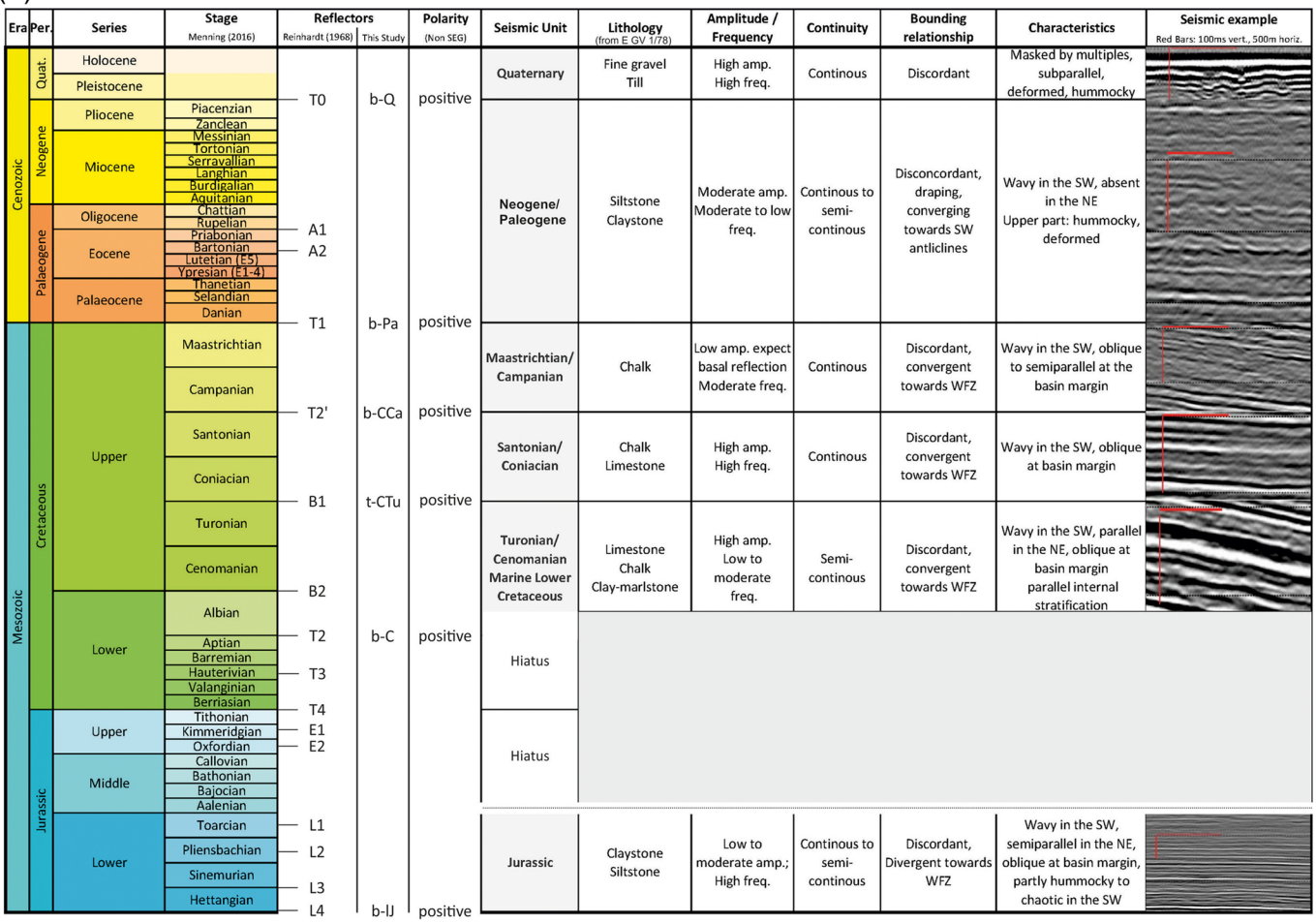

Figure 5a. (a) Seismo-stratigraphic concept for this study. Table summarizes lithology, seismic facies (Prather et al., 1998; Sangree & Widmier, 1979), including amplitude, frequency, continuity, bounding relationships, reflector characteristics, and provides a seismic section example of profile BGR16-254. Exact onset of the hiatus remains unknown. Reflectors in this study are based upon Reinhardt (1993). Stratigraphic table after Menning (2016), size of individual series not scaled to true timespan. b-Q = base Quaternary; b-Pa = base Paleogene; b-CCA = base Upper Cretaceous Campanian; t-CTu = top Upper Cretaceous Turonian; b-C = base Cretaceous; b-lJ = base Lower Jurassic. (b) Continuation of panel (a). Seismo-stratigraphic concept. Reflectors in this study base upon Reinhardt (1993). Stratigraphic table after Menning (2016), size of individual series not scaled to true timespan. ECU = Early Cimmerian unconformity; b-TKe = base Triassic Keuper; b-TMU = base Triassic Muschelkalk; b-TSa = base Triassic Salinarröt; b-TBu = base Triassic Buntsandstein; t-PZAh = top Permian Zechstein anhydrite zone within Leine cyclothem; b-PZ = base Permian Zechstein.

signal penetration with a relatively wide frequency bandwidth with a dominant frequency of 80 Hz. The streamer had an active cable length of 2,700 m with a minimum offset of 33 m. In this study, a major processing task was to remove strong, reverberating multiples caused by the shallow water of the Baltic Sea. We applied a combined strategy consisting of a τ-p domain prestack predictive deconvolution scheme, surface-related multiple attenuation (SRME), and poststack predictive deconvolution to effectively attenuate multiples (Verschuur, 2006). High-amplitude refracted waves were muted. Further processing steps include frequency filtering, amplitude recovery, noise reduction, and poststack time migration. Interval velocities in the study area range from 1,600 m/s (Quaternary) to 5,100 m/s (Zechstein) (Hansen et al., 2007; Noack et al., 2018; Schlüter et al., 1997). This results in a seismic vertical resolution in the order of 5–30 m. Horizontal resolution approximated by the width of the first Fresnel Zone after migration is 20–100 m.

This study focuses on structural and stratigraphic interpretation of a regional reflection seismic profile (BGR16-254) running from the Bay of Mecklenburg toward Rügen Island across the NGB margin into the

(b)

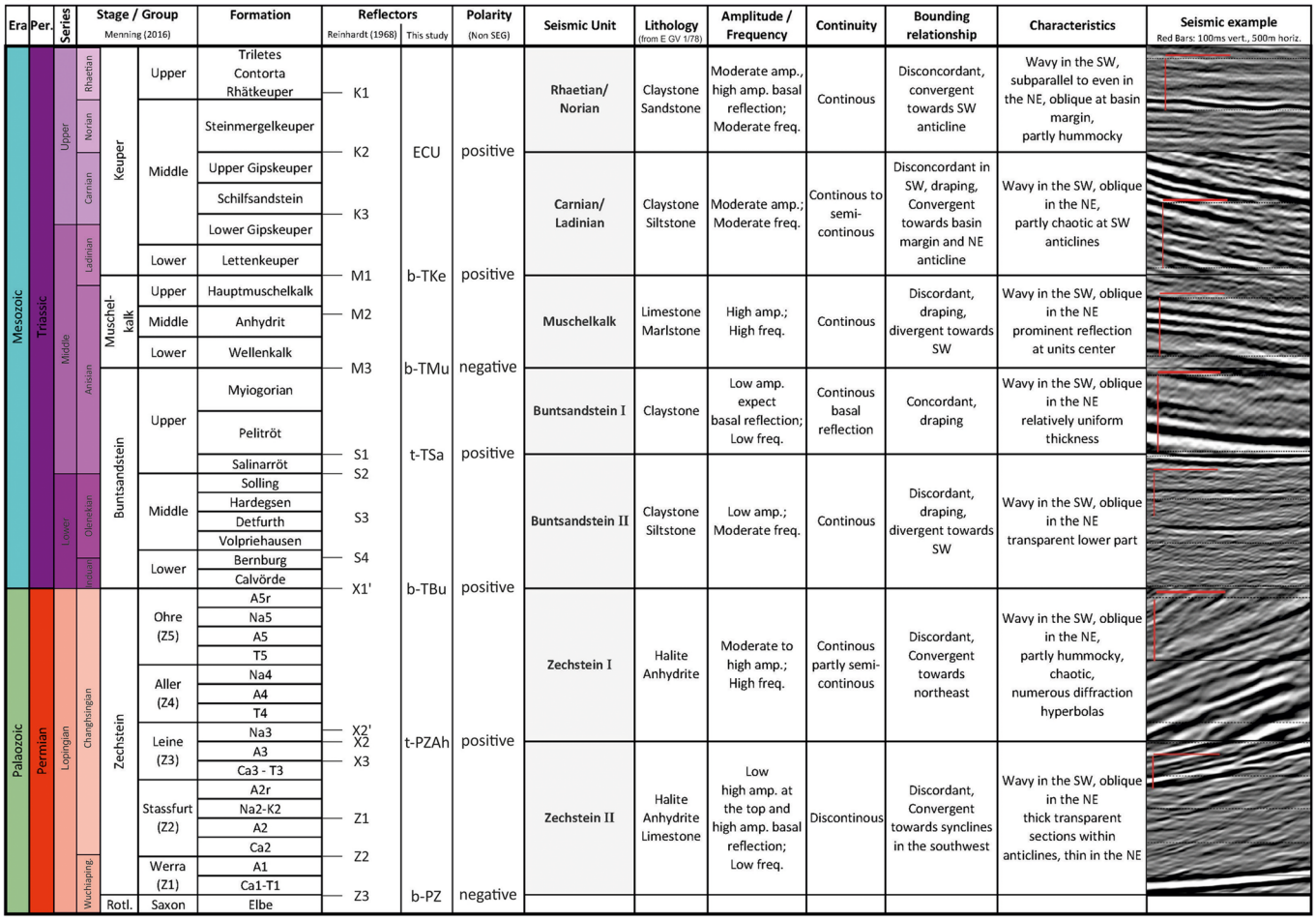

Figure 5b. (continued)

Arkona Basin (Figures 1 and 4). Stratigraphic interpretation of seismic units is based on information from nearby onshore wells (see table in Figure 4). Additionally, we used marine seismic profiles from the Rerik-See area, kindly provided by Neptune Energy (Figure 4), in order to validate our stratigraphic correlation. The well information used in this study comprises well reports of deep research wells and hydrocarbon exploration wells (Hoth et al., 1993; Nielsen & Japsen, 1991; Schlüter et al., 1997). For stratigraphic correlation, most important wells are E Gv 1/78, E WuoRD 6/77, E Pew 1/65, E Pew 2/66, E Dke 1/68, E Rn 2/67, E Rn 3/63, and E Rn 5/66 (Figure 4). Well reports include well markers and in some cases well logs (gamma ray, resistivity, sonic, and density). Lithological information was taken from the detailed geological profiles presented in the well reports. We converted stratigraphic well markers to the time domain using check shot and vertical seismic profiling data for the well-to-seismic tie. Thereby, we considered the position of the well in the structural basin setting to constrain the correlation. Due to the distance to the wells and their different structural positions, stratigraphic correlation is based on thickness, represented by travel time difference, rather than directly upon depth. In addition, the stratigraphic interpretation was linked to results of previous studies (Al Hseinat & Hübscher, 2017; Bachmann et al., 2010; Deutschmann et al., 2018; Hübscher et al., 2010; Kammann et al., 2016; Katzung, 2004; Zöllner et al., 2008).

Thickness in this study is expressed in two-way travel time (TWT) difference between bounding reflectors of a seismic unit. Scaled by seismic velocity, increased travel time difference locally represents increased thickness. Within the two southwestern rim-synclines adjacent to the salt pillows in the Bay of Mecklenburg, we examined local lateral thickness variations (see Figure 4 for location). By the term “local depocenter,” we

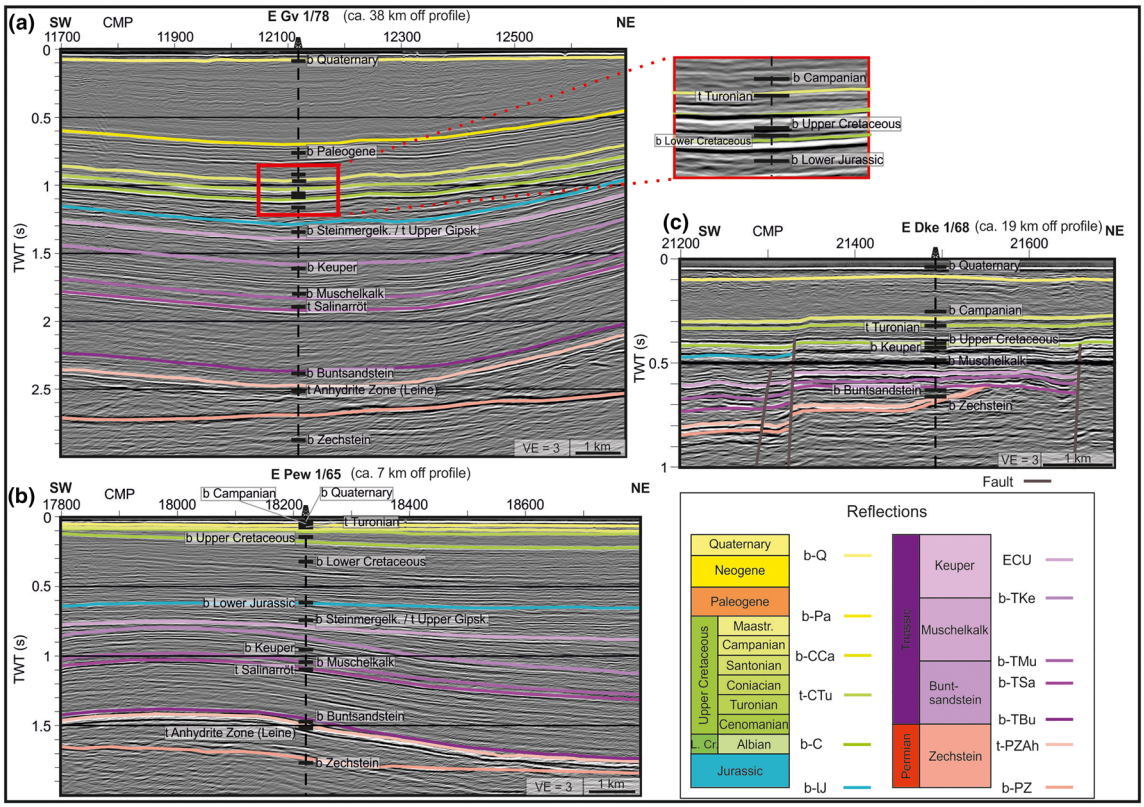

Figure 6. Well-to-seismic tie for wells (a) E Gv 1/78, (b) E Pew 1/65, and (c) E Dke 1/68. For abbreviations, see Figure 5. Well information from Hoth et al. (1993). Location of sections of profile BGR16-254 shown in Figures 1b and 4. "b" = base; "t" = top.

refer to the location of maximum thickness of a seismic unit within the rim syncline (Jackson & Hudec, 2017; Sørensen, 1986). Over time, local lateral thickness variations occur due to salt movement. This causes an interpretable lateral migration in the local depocenter. However, we are aware that this does not necessarily represent the actual depocenter of that specific seismic unit as our analysis bases only on a single time seismic section. Horizon flattening and changing vertical exaggeration helped to identify small local depocenter migrations, although in many cases, an exact location is not distinct. In this case, we picked a location vertically above the previous pick. Hence, the analysis of the local depocenter migration is only qualitative and should be treated with caution. Nevertheless, it was useful to get an idea of local lateral salt flow in the study area.

We developed a seismo-stratigraphic framework for the study area according to the stratigraphic table of Germany (Menning, 2016). The seismo-stratigraphic framework includes 13 post-Carboniferous seismic units (Figure 5). We use the term "seismic unit" for a mappable interval of seismic reflectors, expressed by seismic reflections, whose characteristics differ from those of adjacent seismic units. A seismic unit is bounded by marker reflections, unconformities, or correlative conformities. The interpreted seismic units correspond to Quaternary, Paleogene-Neogene, Maastrichtian-Campanian, Santonian-Coniacian, Turonian to Lower Cretaceous, Jurassic, Rhaetian-Norian, Carnian-Ladinian, Muschelkalk, Buntsandstein I (Myiogorian to Pelitröt), Buntsandstein II (Salinarröt to Calvörde), Zechstein I (Werra to Leine anhydrite), and Zechstein II (Leine anhydrite to Ohre) (Menning, 2016). Figure 5 summarizes the seismo-stratigraphy in this study and provides lithological information based upon the well E Gv 1/78 (Hoth et al., 1993), seismic facies, terminations, key characteristic features of each unit, and a seismic example. Identified bounding reflectors are based upon the seismo-stratigraphic framework in Reinhardt (1993). These are b-Q: base Quaternary; b-Pa: base Paleogene; b-CCA: base Upper Cretaceous Campanian; t-CTu: top Upper Cretaceous Turonian; b-C: base Cretaceous; b-lJ: base Lower Jurassic; ECU; b-TKe: base Triassic Keuper; b-TMU: base Triassic Muschelkalk; b-TSa: base Triassic Salinarröt; b-TBu: base Triassic

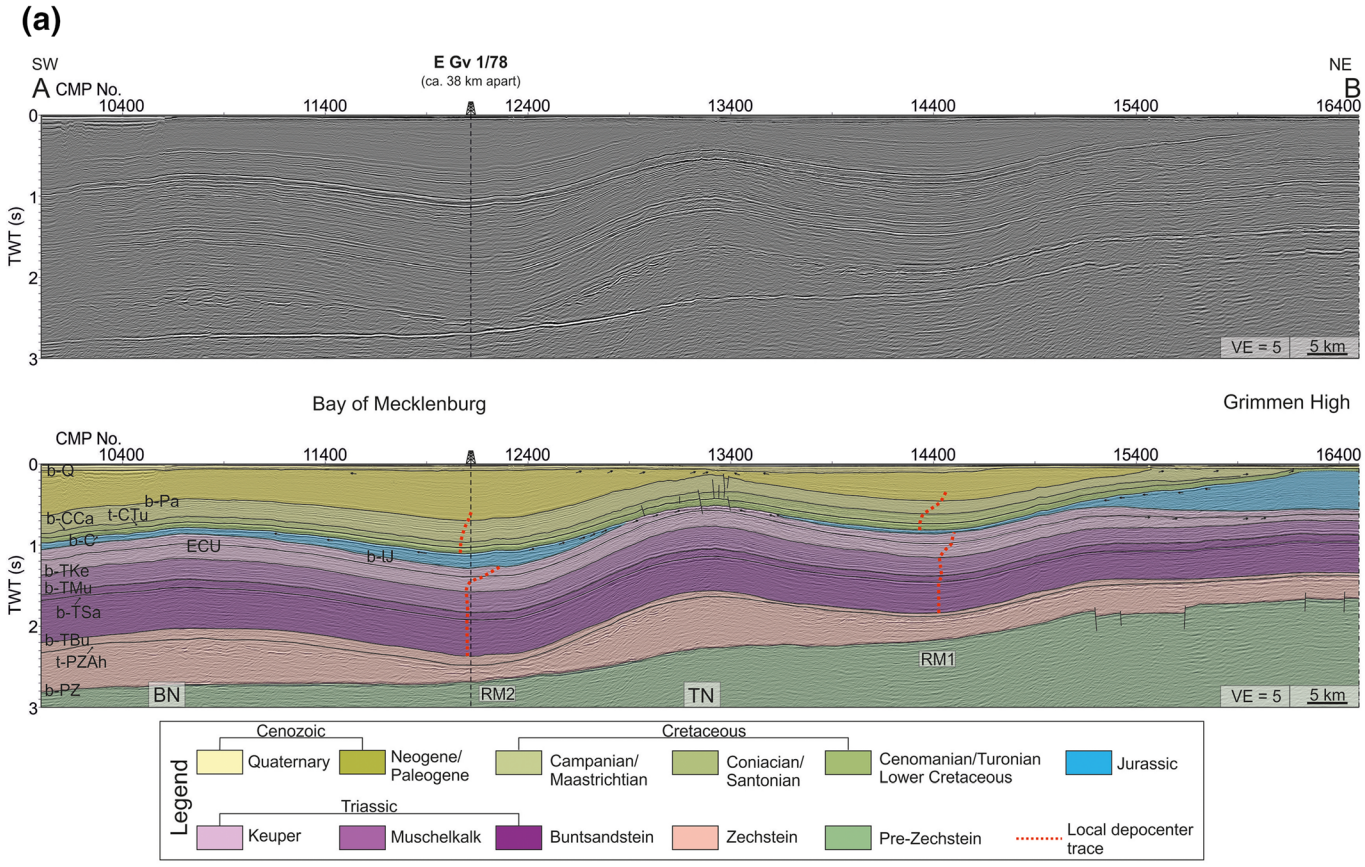

Figure 7a. (a) BGR16-254 time migrated and interpreted section. CMP 10000–16600. The local depocenter trace marks the local position of maximum thickness within specific seismic units. TN = Trollegrund Nord salt pillow; BN = Boltenhagen Nord salt pillow (Reinhold et al., 2008). Location of seismic profile BGR16-254 between A and B shown in Figures 1b and 4. (b) Continuation of Figure 7a. BGR16-254 time migrated and interpreted section. CMP 16600–23000. F = fault; PR = Prerow salt pillow (Reinhold et al., 2008). Location of seismic profile BGR16-254 between B and C shown in Figures 1b and 4.

Buntsandstein; t-PZAh: top Permian Zechstein Anhydrite Zone within Leine cyclothem; and b-PZ: base Permian Zechstein.

4. Observations

4.1. Stratigraphic Units and Well Correlation

Figure 6 shows examples of the well-to-seismic tie for the wells E Gv 1/78, E Pew 1/65, and E Dke 1/68. The Zechstein seismic unit is the deepest unit imaged in this profile (Figures 1b and 6). The base Zechstein well marker of E Gv 1/78 does not match the seismic reflector since the well is situated in the deeper part of the basin (Figures 6 and 4). For the wells E Pew 1/65 and E Dke 1/68, the well markers and base Zechstein reflector (b-PZ) coincide (Figures 6b and 6c). The base Zechstein is overlain by a reflection free area, which represents the Stassfurt (Z2) cyclothem. It is bound at the top by hummocky to chaotic high amplitude reflections (Figures 6a and 7). They correlate with the main anhydrite sequence in the Leine (Z3) cyclothem. The top of this unit is marked by the Leine anhydrite zone reflector (t-PZAh). Toward the basin margin, thickness of the Zechstein II (Werra to Leine anhydrite) unit decreases (Figure 7). This results in a thin Zechstein unit with high-amplitude bounding reflectors. Toward the basin margin, the Ohre and Aller cyclothems pinch out (Figures 3 and 7). The Zechstein terminates against the base Buntsandstein reflector (b-TBu) closely to the Wiek Fault in this profile (Figure 7b).

The basal reflector (b-TBu) of the Buntsandstein II (Salinarröt to Calvörde) unit is in agreement with the depth of all three well markers (Figure 6). Reflection amplitude in the southwest profile part is low due to

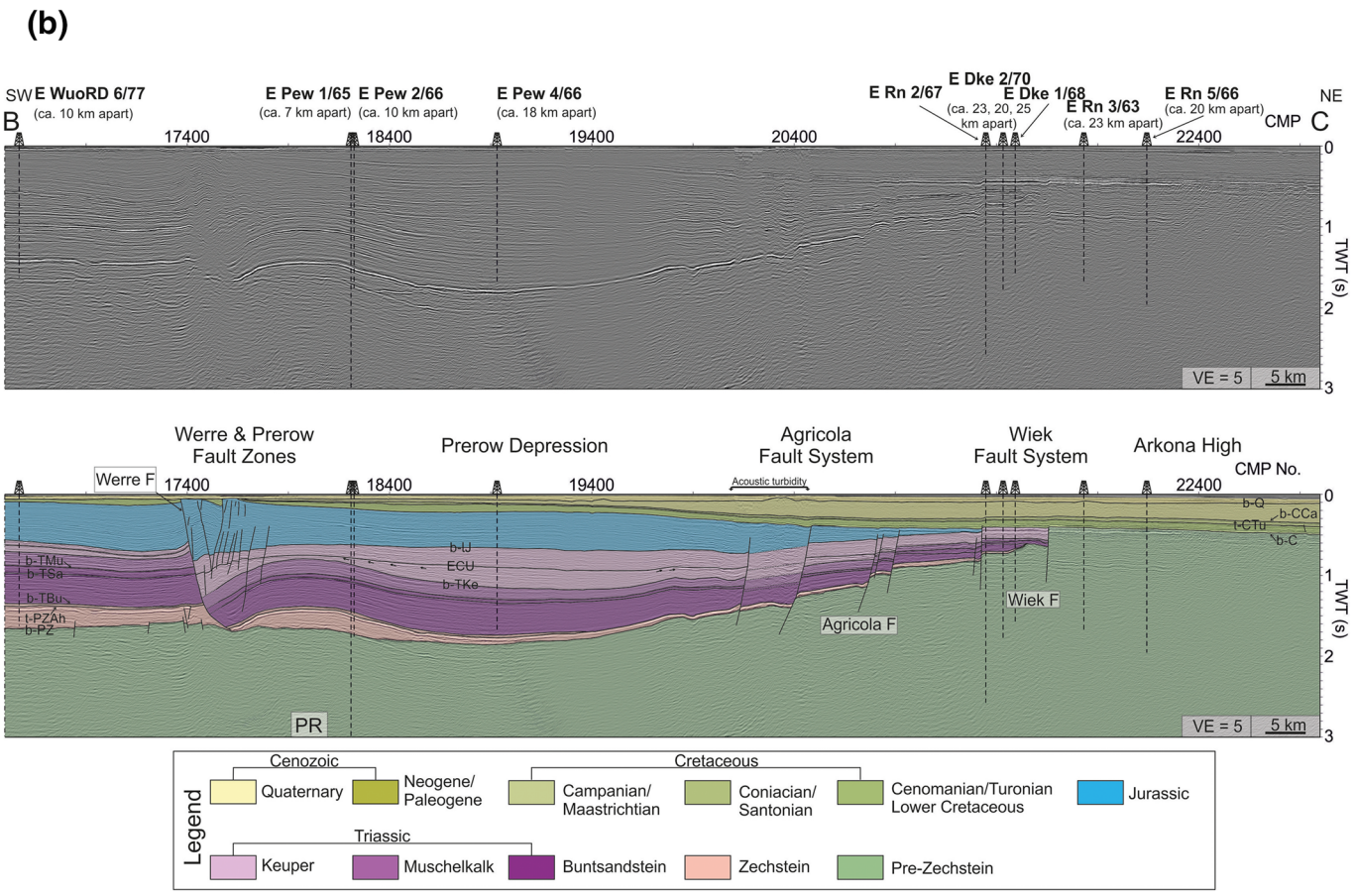

Figure 7b. (continued)

the small seismic velocity contrast between compacted Triassic claystone and underlying halite of the Zechstein Ohre cyclothem (Figure 7a). The Buntsandstein II unit shows maximum thickness in the southwest. Thickness of the unit decreases toward the basin margin, where it terminates close to the Wiek Fault in an onlap against the Zechstein. The Buntsandstein I unit (Myogorian to Pelitröt) shows a high-amplitude basal reflector (t-TSa), which corresponds with the top of anhydrite deposits in the Salinarröt succession marked in the wells (Figure 6). Well markers correspond with the low-amplitude base Muschelkalk (b-TMu) reflector (Figure 6). Intercalated limestone and anhydrite within the Middle Muschelkalk create a set of prominent reflectors (Figure 7). We subdivide the overlying Triassic Keuper into an upper Rhaetian-Norian seismic unit overlying the lower Carnian-Ladinian unit. The ECU, marking the top Upper Gipskeuper at the base Norian, separates these units (Figures 5 and 7). Toward the basin margin, the Carnian-Ladinian seismic unit pinches out (Figure 7b). Here, Muschelkalk lime-marlstones form the ECU subcrop and create a high impedance contrast. Well markers and the ECU and base Keuper reflectors match in the Bay of Mecklenburg (Figure 6).

Likewise, well markers are in agreement with the base Lower Jurassic (b-lJ) reflector. The Jurassic terminates as a toplap northeast of the AFS (Figure 7b).

The base Cretaceous reflector (b-C) is in agreement with the base Upper and Lower Cretaceous markers in the wells (Figure 6). Thickness of the Lower Cretaceous Albian at the basin margin is 9 m (E Dke 1/68) and therefore below seismic resolution. A distinct base Lower Cretaceous reflector is not observed (Figures 6 and 7). The well E Pew 1/65 shows a Lower Cretaceous thickness of 125 m with 110 m of pre-Albian sediments. In the nearby E Pew 4/66 well, the Lower Cretaceous consists of only 8 m of Albian sediments. Hence, the locally increased thickness in the E Pew 1/65 well is very isolated as no pre-Albian Lower Cretaceous sediments were drilled in the surrounding wells. Deutschmann et al. (2018) interpreted a base Lower Cretaceous

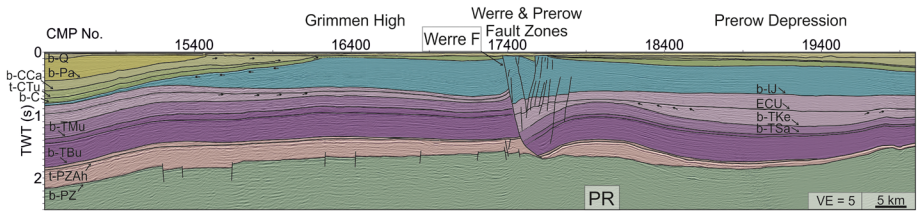

Figure 8. Interpreted central part of profile BGR16-254; see Figure 1(b) for location.

reflection, however, with noting that it is mainly transparent. The increased thickness in the E Pew 1/65 well could be either fault related, since it was drilled between the Werre and Prerow fault zones (Deutschmann et al., 2018), or more likely the result of incorrect dating as also concluded by Hübscher et al. (2010) (Figure 4).

The top Turonian reflector (t-CTu) corresponds closely with the marker in all three wells (Figure 6). The overlying Santonian-Coniacian seismic unit is bound by the base Campanian reflector (b-CCA) and is truncated by the Quaternary at the flanks of the Grimmen High (Figure 8). The base Campanian reflector (b-CCA) separates a less to higher stratified reflection pattern, which correlates to the base Campanian marker in the wells E Gv 1/8 and E Dke 1/68. In the well E Pew 1/65, thickness of the Campanian is decreased. At the Grimmen High, the reflector terminates in an onlap against the top Turonian (Figure 8). From the Grimmen High toward the SW, thickness of the Maastrichtian-Campanian unit increases, and reflectors are divergent.

The overlying Neogene-Paleogene seismic unit terminates as a toplap against the Quaternary in the Grimmen High area (Figure 8). The base-Paleogene (b-Pa) reflector corresponds with the well marker of the well E Gv 1/78 (Figure 6a). The angular unconformity of the base Quaternary correlates with the base of glacial deposits, which overlie Cenozoic clay in the E Gv 1/78 and Cretaceous chalk in the wells E Pew 1/65 and E Dke 1/68.

4.2. Faults

In the southwest part of the analyzed seismic profile, above the Trollegrund Nord (TN) salt pillow, a set of crestal faults dipping toward the anticline center pierce the Upper Cretaceous and eventually die out within the Keuper (Figure 7a).

In the central part of the profile (Figure 7b, WFZ), a prominent NE dipping listric fault dissects almost the entire sedimentary cover from the Zechstein to the Quaternary. It was identified as the Werre Fault in the literature (e.g., Deutschmann et al., 2018). Normal faults pierce the base of the Zechstein in this area. In the overburden, additional synthetic normal faults as well as a set of antithetic normal faults characterize the WFZ. Normal faults in the SW part of the hanging wall form Y-shaped grabens, while toward the northeast, normal faults dip SW. A precise analysis of fault displacement is difficult for the WFZ as reflectors are difficult to trace. The Buntsandstein and Muschelkalk units show constant fault displacement at the Werre Fault and constant thickness in the hanging wall. Thickness is increased in the Keuper and Jurassic. Reflectors in these units show a divergent pattern toward the Werre Fault, which indicates the extensional phase of activity of this fault zone. The base Cretaceous in the hanging wall of the Werre Fault is located above the corresponding reflector in the footwall (Figure 8).

A set of listric faults in the northeast part of the profile correspond geographically with the AFS (e.g., Deutschmann et al., 2018) (Figures 7b). One of them could be identified as the Agricola Fault. All faults dip SW and pierce the pre-Zechstein to Jurassic successions. These faults show quite constant throw in the Zechstein, Buntsandstein, and Muschelkalk units. Fault displacement decreases in the Keuper and Jurassic and vanishes in the Cretaceous units. Further northeast, we identified the Wiek Fault (Krauss & Mayer, 2004; Seidel et al., 2018). Beyond this fault, Triassic deposits are either absent, too thin to be resolved, or masked by multiples.

4.3. Local Depocenter Analysis

The two rim-synclines in the Bay of Mecklenburg reveal a local, lateral migration when comparing the local depocenter trace (Figures 7a, red dotted lines). For the Buntsandstein and Muschelkalk successions in the

RM1 rim syncline, the local depocenter trace is nearly vertical. Within the Carnian-Ladinian successions, a NE migration of the local depocenter becomes visible. This NE migration continued with less displacement within the Norian-Rhaetian until the base Jurassic. The Jurassic is only preserved as a thin erosional remnant, which hampers the depocenter analysis. The Cretaceous Santonian-Coniacian local depocenter was relocated further SW. It gradually migrated NE during the Santonian-Coniacian. Within the Maastrichtian-Campanian, the local depocenter migrated further NE with enhanced displacement. In the lower Cenozoic successions, the migration of the local depocenter trace decreases slightly. In the upper part, it is no longer traceable. In total, we observe a migration of ~880 m from Keuper to Jurassic times and 1.5 km from the Cretaceous to Cenozoic within the RM1 rim syncline.

We observe similar variations at the RM2 rim-syncline (Figures 7a). The location of the local depocenter remained fixed in the Buntsandstein and Muschelkalk. In the Keuper Carnian-Ladinian unit, the local depocenter began migrating NE. Migration persisted with a relatively large displacement within the Norian-Rhaetian. However, the overall thickness variations in this area are minor, which limits accuracy. The Cretaceous local depocenter was relocated further SW, and there is no observable lateral migration from Cenomanian to Santonian times. Within the Maastrichtian-Campanian, the depocenter trace shows a continuous NE migration within the unit until the lower Cenozoic. In total, we interpret a lateral migration of roughly 2 km from Keuper to Jurassic times and ~875 m within the Late Cretaceous within the RM2 rim syncline. However, the observed 2 km of lateral migration in the Keuper seems rather large. Thickness variations within the RM2 rim-syncline Keuper succession are small, which hampers a precise identification of the local depocenter. Therefore, the real lateral migration is especially uncertain in this area.

5. Interpretation and Discussion

In this chapter, we discuss the interpretation of regional tectonic structures in terms of their thick-skinned or thin-skinned character. Thick-skinned deformation involves the subsalt successions and/or basement in an extensional (Vendeville & Jackson, 1992) or compressional setting (Coward, 1983). In the presence of a detachment layer, for example, caused by salt, deformation is decoupled in the underlying and overlying successions. Thin-skinned deformation refers to deformation within the detachment layer and its overburden either in an extensional or compressional tectonic regime (Coward, 1983; Vendeville & Jackson, 1992). In the following, we analyze the timing and activity of faults and salt structures imaged on our seismic profile, describe their thick- or thin-skinned characteristics, and discuss potential salt pillow growth mechanisms within the regional geological context. In this study, by thick-skinned faults, we refer to faults rooted in the pre-Zechstein successions.

5.1. Thick-Skinned Deformation

Major faults intersect the Zechstein succession in the northeast part of the profile (Figure 7). Faults of the Wiek Fault System and AFS are thick-skinned as they dissect the entire Jurassic, Triassic, and Zechstein successions and are rooted within the sub-Zechstein. In the WFZ, we interpret the main Werre Fault as NE dipping listric fault, which dissects the Jurassic and Triassic. However, it is detached near the base Zechstein. Faults piercing the base Zechstein could indicate that the fault zone is affected by thick-skinned deformation; however, its main components are thin-skinned.

Thicknesses of the Zechstein, Buntsandstein, and Muschelkalk units shown in the profile gradually increase in southwest, basinward direction. This implies increased subsidence toward the basin center, most pronounced in the Buntsandstein (Figure 7). These observations are in accordance with previous studies and the concept of thermal subsidence from Permian to Middle Triassic times. Subsidence was highest in the basin center, which led to thicker sedimentary infill with Zechstein, Buntsandstein, and Muschelkalk deposits (Scheck & Bayer, 1999; van Wees et al., 2000; Ziegler, 1990) (Figure 9a).

Lower and, partly, Middle Keuper units are absent at the northeast basin margin in this profile (Figures 7b). Falling sea levels during the Carnian and resulting falling sedimentation base levels affected the sedimentation during this time (Katzung, 2004; Ziegler, 1990). This explains the observed lack of Lower to Middle Keuper sediments caused by nondeposition and erosion along the relatively higher area of the Rügen Swell and Arkona High (Figures 7b). Here, the ECU directly overlies the Muschelkalk unit. In southwest direction, toward the Bay of Mecklenburg, Lower Keuper and Middle Keuper units build the ECU subcrop. This trend coincides with the ECU subcrop map (Figure 4) and allows the correlation of the ECU reflector.

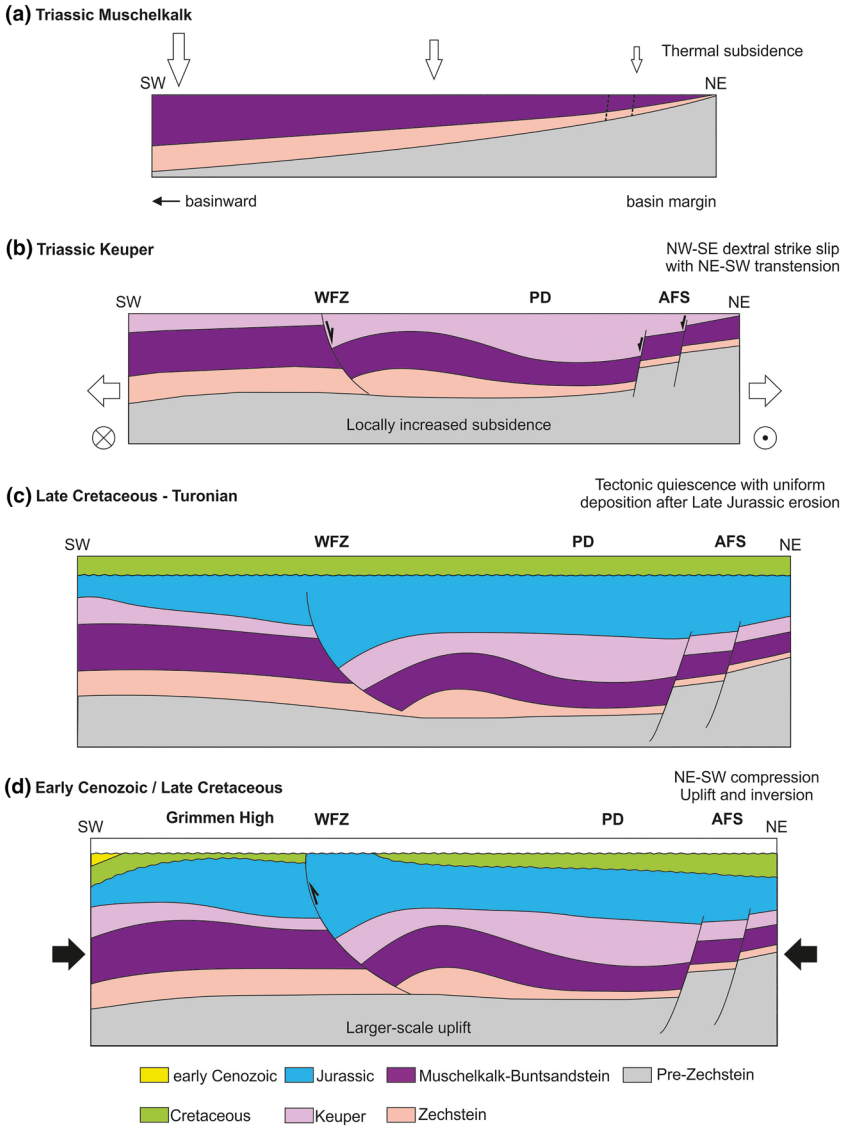

Figure 9. Sketch illustrating the tectonic evolution at the northeastern North German Basin margin as derived from the presented analysis of profile BGR16-254.

Therefore, its deposition marks the end of a stratigraphic gap from the top Upper Gipskeuper (Weser Formation, close to the base Norian) to base Steinmergelkeuper (Arnstadt Formation, in the Norian) (Beutler et al., 2005). The ECU erosionally truncates Carnian-Ladinian reflectors in a toplap at the Grimmen High and at the NE flank of the Prerow salt pillow (Figure 8, CMP 15400–16400). We associate this with the falling sea level during the Carnian (Katzung, 2004). However, the stronger erosion between the Grimmen High and Prerow salt pillow suggests that this area experienced less subsidence.

The AFS is characterized by a set of SW dipping normal faults on this seismic transect (Figure 7b). Thickness of the Buntsandstein and Muschelkalk is uniform within the hanging wall and footwall of the Agricola Fault. The Carnian-Ladinian seismic unit within the hanging wall appears increased and fault throw along the Agricola Fault decreased from ~40 ms at the base Keuper to ~11 ms at the ECU. However, as the seismic data are in time, true fault throw is scaled by velocity and might be larger than visible in the data. The Rhaetian-Norian seismic unit shows increased thickness in the hanging wall with slightly divergent reflections. This indicates syndepositional faulting in the Late Triassic (Figures 7b). Within the Prerow Depression, deposits of the Carnian-Ladinian as well as Rhaetian-Norian units show increased thickness and reach a local maximum (Figure 7b). Comparing this to Keuper thickness further southwest,

maximum Keuper thickness almost doubled in the Prerow Depression and reaches ~650 m (480 ms TWT; ~2,700 m/s; Schlüter et al., 1997). This indicates that the Prerow Depression experienced subsidence during the Late Triassic and formed a local basin bound to the northeast by the contemporaneous active AFS, which was also stated by Deutschmann et al. (2018) (Figure 9b). Active faulting and subsidence in the Carnian were coeval with E-W to ENE-WSW extension, related to accelerated activity in the North Sea rift system and Glückstadt Graben (Ziegler, 1990). At the Carnian-Norian transition, rifting activity decreased (Schröder, 1982; Ziegler, 1990), and further subsidence within the Rhaetian-Norian is difficult to relate to normal faulting caused by E-W extension. However, increased Rhaetian-Norian thickness suggests ongoing faulting and subsidence in the Prerow Depression. We interpret this in accordance to the results of Krauss and Mayer (2004) and Deutschmann et al. (2018), who associated faulting within the AFS with the reactivation of Middle Devonian-Early Carboniferous faults during the Late Triassic and the contemporaneous formation of other fault zones included in the Western Pomeranian Fault System. These faults were induced by NW-SE dextral strike slip movements within the Trans-European Suture Zone, which were accompanied by approximately NE-SW directed transtension (Erlström et al., 1997; Seidel et al., 2018). Faults of the AFS strike ~NNW-SSE, which is almost perpendicular to the main extensional stress. Therefore, a reactivation of these faults is likely and could explain subsidence in the adjacent Prerow Depression (Figure 9b). Indications of a general uplift of the Baltic Shield and corresponding influx of clastics during the Rhaetian (Erlström et al., 1997) fit this structural evolution by providing sufficient local basin fill.

Around Rügen, the Jurassic gradually thickens along the AFS and Prerow Depression toward the WFZ and Grimmen High (Figure 7b). Fault throw in the AFS further decreased suggesting syntectonic deposition and ongoing subsidence of the Prerow Depression. In the Bay of Mecklenburg, the Jurassic unit is strongly reduced and preserved strata concentrates in the rim synclines. Uplift related to the Middle-Late Jurassic North Sea doming event (Graversen, 2006; Underhill, 1998; Ziegler, 1990) caused erosion of most of the Jurassic, in some extent even Upper Triassic strata, from westward direction in the Bays of Kiel and Mecklenburg (Al Hseinat & Hübscher, 2017; Hansen et al., 2005, 2007; Hübscher et al., 2010). The thinned Jurassic unit in the Bay of Mecklenburg corresponds with this interpretation. However, the preservation of thicker Jurassic deposits in the Prerow Depression suggests ongoing subsidence and thereby a different origin. Due to its closer position to the basin margin, the Zechstein successions in the Prerow Depression lack large amounts of mobile halite (Figures 3 and 7b). Therefore, we expect the effect of salt movement on lateral thickness variations in this area to be minor. However, modeling results by Hansen et al. (2007) show a locally increased tectonic subsidence in this area. Similar to Deutschmann et al. (2018), we explain the increased subsidence and subsequent deposition of the Jurassic in the Prerow Depression by ongoing normal faulting in the AFS related to transtensional movements at the Trans-European Suture Zone (Figure 9c). The listric SW dip of the Agricola Fault suggests rotational block faulting possibly caused by increased basement tilt. This is in accordance to basement subsidence rates calculated by Kossow and Krawczyk (2002), which show relatively higher subsidence rates toward the basin center from the Late Permian to Late Triassic. This suggests a deepening of the basin resulting in increased basement tilt in the Late Triassic and Jurassic. This could explain locally increased subsidence at the basin margin above the rotated hanging walls of deep-seated basin margin faults, which could be detached near the Paleozoic basement (Krawczyk et al., 2002).

Apart from the area of the WFZ, the Turonian-Cenomanian-Lower Cretaceous unit has uniform thickness along the profile (Figure 7). Major faulting is absent. We interpret this in accordance to Kossow and Krawczyk (2002), Kley and Voigt (2008), Hübscher et al. (2010), and Al Hseinat and Hübscher (2017) as a period of tectonic quiescence and rising sea levels lasting from the Albian transgression until the Coniacian (Figure 9c). Thickness of the Santonian-Coniacian unit slightly decreases from the northeast toward the WFZ (Figures 7b and 8). From the southwest toward the Grimmen High, thickness of the Santonian-Coniacian unit decreases, and the base Campanian (b-CCA) onlaps to the Turonian-Lower Cretaceous. This indicates synkinematic deposition and the onset of uplift of the Grimmen High (Figure 8). The Maastrichtian-Campanian unit is convergent with thinned deposits at both the NE as well as the SW flank of the Grimmen High. At its center, the Maastrichtian-Campanian is completely eroded, which suggests intensified uplift (Figure 9d). It is a clear indication for the onset of the basinwide inversion phase in the Late Cretaceous and coeval uplift of the Grimmen High (Kley, 2018; Kley & Voigt, 2008) (Figure 9a). In contrast to Kossow and Krawczyk (2002) and Deutschmann et al. (2018), we observe a thin

Late Cretaceous remnant above the Grimmen High due to the improved imaging of shallow successions. This suggests that the seismic profile images the western boundary of the Grimmen High. Taking the Cretaceous succession at the northeast end of the profile as a reference and assuming it did not experience erosion, thickness at the Grimmen High prior to inversion was ~460 m (430 ms TWT, 2,150 m/s; Schlüter et al., 1997). This represents a relative uplift of ~460 m. Kossow and Krawczyk (2002) calculated the amount of erosion and relative uplift to ~500 m. The authors however stated higher internal velocities for the Cretaceous ranging from 2,000 to about 3,300 m/s. Assuming an average velocity of 2,650 m/s yields a relative uplift of 570 m for our data. Accordingly, the observed amount of uplift in this study is in agreement with results of Kossow and Krawczyk (2002).

Kossow et al. (2000) and Kossow and Krawczyk (2002) interpreted the Grimmen High as a drag-related anticline forming a fault-bend-fold geometry due to northward increasing resistance against overburden deformation. As a cause, the authors mention the pinch out of the decoupling Zechstein units, which caused increasing basal friction and resulted in up-thrusting of the overburden onto the basin edge. The authors suggested a possible strike slip and transpressive component based upon the similarity with a positive flower structure. In principle, this study confirms the uplift of the Grimmen High starting within the Coniacian-Santonian and intensifying in the Campanian-Maastrichtian. However, we propose that the tilted basin margin configuration with the Prerow Depression and AFS affected the uplift in the Baltic sector of the NGB. NE-SW directed shortening possibly inverted southwest dipping older extensional faults at the northeastern basin margin. This induced reverse faulting partially decoupled by the Zechstein salt. Compressional deformation caused uplift of rotated basement blocks and was distributed within the overburden causing uplift and erosion of the Cretaceous in the area of the Grimmen High and Prerow Depression (Figure 9d).

5.2. Salt Tectonics and Thin-Skinned Deformation

In this study, the analysis of thin-skinned deformation deals with the detaching salt layer and its supra-salt cover. Our analysis mainly focuses on thickness variations and faulting of the overburden due to local lateral salt flow. The location of maximum thickness of an individual unit corresponds with the local depocenter during this time, and we interpret a lateral migration as a consequence of lateral salt movement.

The observed internal seismic layering of the Zechstein unit with a lower rather reflection free part, which indicate halite rich formations, and a high-amplitude upper part corresponding with anhydrite rich successions at the top is in good accordance with the Zechstein stratigraphic framework (Figures 7) (Katzung, 2004; Strohmenger et al., 1996; Tucker, 1991; Warren, 2008). The t-PZAh reflector marks the transition from intercalated anhydrite within the Leine (Z3) salt to the main anhydrite formation of the Leine cyclothem (Figures 5 and 7). The high-amplitude but disrupted reflections within the anhydrite zone indicate internal deformation including boudinage and folding of the anhydrite layers similar to the Z3 stringer observed in the Netherlands (Strozyk et al., 2012; van Gent et al., 2010). The underlying thick, almost reflection free area of the Lower Zechstein unit accordingly corresponds with the Stassfurt and Werra cyclothem. Well information suggests that its major portion is Stassfurt halite (Figures 3 and 7a). Northeast of the WFZ, thickness of the Zechstein decreases accompanied by a facies change due to decreasing amounts of halite and anhydrite toward the basin margin (Katzung, 2004). In the Rügen area, the high-amplitude reflection characterizing the Zechstein seismic unit corresponds with increasing amount of carbonates, especially of the Stassfurt cyclothem (Kaiser, 2001; Katzung, 2004; Zagora & Zagora, 1997).

5.2.1. Thin-Skinned Deformation in the WFZ

The Werre Fault has a listric NE dipping shape with thinned Zechstein salt in the hanging wall and a folded overburden. We interpret this as a rollover structure. Both the Carnian-Ladinian and Rhaetian-Norian seismic units show increased thickness northeast of the fault. This marks the infill of the syndepositional half graben (Figure 9b). Many normal faults dip toward the center of the halfgraben. They were created in response to the subsiding hanging wall of the Werre Fault. This evidences the initiation of normal faulting at the Werre Fault during the Late Triassic. The development of the half-graben continued during the Early Jurassic indicated by the increased thickness of the Early Jurassic seismic unit (Figures 7b and 9c).

To the northeast, this area is connected to an anticline associated with the Prerow salt pillow (Reinhold et al., 2008; Pr in Figure 7b and salt structure adjacent to E Pew 1/65 well in Figure 4). Deutschmann et al. (2018) made similar observations based upon seismic profiles closer to the coast. Here, the Prerow

salt pillow is more pronounced. However, the anticline on our profile is mainly caused by the absence of salt within the WFZ than actual salt accumulation, as Zechstein thickness southwest of the WFZ and within the anticline is nearly equal, though the anticline on our profile could represent the edge of the Prerow salt pillow. Further, the absence of salt in the WFZ could be caused by out of plane salt flow possibly accumulating in the SE located central part of the salt pillow. Modeling results of Hansen et al. (2007) show a SE increase in Zechstein thickness toward Rügen along the Werre Fault, which is in accordance with our interpretation. The general increase of Zechstein thickness southwest of Rügen Island shown by Hansen et al. (2007) can be explained by increased primary thickness due to proximity to the basin center (Kossow et al., 2000) as the basin margin bends northeast along southern Rügen Island (Katzung, 2004). Therefore, we interpret only a local, minor fault-controlled salt flow between the WFZ and Prerow Fault Zone.

The exact timing of the initialization of the WFZ is an aspect of recent discussion. Krauss and Mayer (2004) referred to the Werre and Prerow fault zones as a system of NNW-SSE trending pull-apart graben structures due to Early Cimmerian (Late Triassic) reactivation of basement faults of Caledonian and Variscan origin. Al Hseinat and Hübscher (2017) mention that the E-W directed extensional tectonic regime affecting the NGB reactivated deep-rooted basement faults in this area. Deutschmann et al. (2018) proposed transtensional movements due to Cimmerian tectonics during the Late Triassic to Early Jurassic and the formation of a roll-over structure. Observations by Seidel et al. (2018) northeast of Rügen agree with Krauss and Mayer (2004). They associate the WFZ with en echelon structures of the Western Pomeranian Fault System, which developed during Mesozoic extensional tectonics. In principal, our observations agree with recent studies but, however, allow a more precise timing and complete image of the fault zone. Our observations of active normal faulting in the Carnian-Ladinian, Rhaetian-Norian, and Jurassic seismic unit suggest that the initialization of the WFZ was coeval with extension in the Late Triassic-Early Jurassic and corresponding active faulting in the AFS and subsidence in the Prerow Depression (Figures 9b and 9c). Decoupled by the mobile Zechstein salt, thin-skinned normal faulting at the approximately NW-SE striking Werre Fault was caused by NW-SE dextral strike slip movements and associated NE-SW directed transtension within the Trans-European Suture Zone (Deutschmann et al., 2018; Krauss & Mayer, 2004; Seidel et al., 2018). During Late Cretaceous basin inversion, the NE-SW compressional stress orientation was perpendicular to the NW-SE trending Werre Fault, which made the fault especially prone to reactivation (Al Hseinat & Hübscher, 2017; Seidel et al., 2018). The associated compression reactivated the Werre Fault resulting in the displacement of the base Cretaceous reflector in the hanging wall above its counterpart in the footwall (Figure 9d). The related uplift caused erosion of almost the entire Cretaceous successions over an ~3 km-wide area northeast of the Werre Fault. Accordingly, this study provides a reinterpretation of the WFZ as an inverted thin-skinned normal fault system.

The Prerow Fault Zone as mapped by Deutschmann et al. (2018) further southeast is not visible in our seismic data, which was acquired further to the northwest. Probably, the Prerow Fault Zone merges with the WFZ to a combined fault system in this area.

5.2.2. Timing of Salt Movement in the Bay of Mecklenburg

In the Bay of Mecklenburg, two salt pillows are imaged by our profile, namely, the TN and Boltenhagen Nord (BN) pillows (Figure 4) (Reinhold et al., 2008). Both analyzed depocenter traces within the adjacent rim synclines (RM1 and RM2, Figures 7b) nearly vertically transect the Buntsandstein and Muschelkalk successions, and no local thickness variations are observable. Hence, salt movement was not yet triggered, which is in accordance to previous studies (Al Hseinat & Hübscher, 2017; Hübscher et al., 2010; Kossow et al., 2000; Zöllner et al., 2008).

The NE migration in the depocenters and thinning of the Keuper toward the pillow crest evidence the initiation of salt movement and pillow growth during deposition of the Keuper. The starting of the NE migration of the local depocenter traces suggests a Carnian-Ladinian triggering. However, larger Norian-Rhaetian thickness variations within the RM1 rim syncline beneath the overlaying thin Jurassic unit indicate that the main phase of salt flow was during the Norian-Rhaetian (Figures 7a). Therefore, this study allows a more precise timing than the previously stated Late Triassic initiation (Al Hseinat & Hübscher, 2017; Hübscher et al., 2010; Kossow et al., 2000; Zöllner et al., 2008). This timing correlates with the initiation of many other salt structures in the southern part of the NGB (Jaritz, 1973; Meinhold & Reinhardt, 1967; Rühberg, 1976) and within the Polish Basin (e.g., Krzywiec et al., 2017).

The Jurassic sequence is strongly eroded in the Bay of Mecklenburg. This hampers interpretation of salt movement during this time and requires consideration of additional adjacent seismic profiles. However, thicker remnants of Jurassic strata are preserved in both rim synclines (Figure 7a). Uplift in the Jurassic and resulting erosion occurred on a larger scale as discussed in section 5.1. Therefore, assuming a local similar degree of erosion above the pillow crest and rim synclines during the Jurassic, we suggest that thickness of the Jurassic was increased within the rim synclines prior to erosion. This indicates ongoing salt pillow growth at least in Early Jurassic times. Thickness is uniform within the Lower Cretaceous to Turonian. Therefore, we interpret a cessation of local salt flow during this time.

Changed depositional regimes possibly affected by basement tilt, as described in section 5.1, relocated the local depocenter traces in the Late Cretaceous (Figures 7a). The observed NE depocenter migration in both rim synclines marks a phase of renewed salt flow and pillow growth beginning in the Santonian-Coniacian and lasting until the Cenozoic. Local thinning of the Upper Cretaceous successions toward the TN pillow center is overprinted by the general SW thickness increase caused by uplift of the Grimmen High (Figure 8). A set of normal faults piercing the Cretaceous above the pillow crest remind of a crestal collapse graben structure. We associate this with overburden extension and bending as a result of rising salt. The Cenozoic is clearly thinned above the TN pillow while thick successions within both rim synclines express ongoing salt movement. When exactly salt movement ceased is an aspect of future work and requires a detailed stratigraphic subdivision of the Cenozoic.

In summary, we observed two phases of salt movement, which are coeval with phases of increased regional tectonic stress. Initiation of salt pillow growth was in the Late Triassic (mostly Rhaetian-Norian) with movement lasting at least throughout the Early Jurassic. During this time, the study area was affected by extension. The second phase took place from the Santonian-Coniacian until the Cenozoic. It correlates to the onset of the Africa-Iberia-Europe convergence and resulting phase of basinwide inversion, the change of the regional stress field from extensional to compressional and associated uplift of the Grimmen High.

5.2.3. Pillow Growth Mechanisms

In a literature-based compilation, Warsitzka et al. (2018) summarized the salt tectonic evolution of the Southern Permian Basin and mapped potential trigger mechanisms that caused salt structure initiation. For the northeastern NGB margin, their compilation suggests a triggering either by gravity gliding or by thin-skinned or minor basement involved extension. However, the referenced studies were rather speculative and partly far away from the actual basin margin in the Baltic Sea sector. In the following, we revise potential trigger and salt pillow growth mechanisms for our study area and discuss their compatibility with the regional tectonic interpretation described above (Figure 10). Besides the mechanisms mentioned by Warsitzka et al. (2018), we further consider for completeness salt pillow growth driven by differential loading or basement-involving faulting.

A basement involving fault-controlled salt structure evolution (as in Jackson et al., 1994; Steward & Coward, 1996; Withjack & Callaway, 2000 Warren, 2008) (Figure 10b) is well known to have created salt anticlines above basement faults in the Southern Permian Basin, for example, in the Glückstadt Graben, and in other basins such as the Levant Basin (e.g., Kockel, 1999; Reiche et al., 2014; Warren, 2008; Warsitzka et al., 2018). However, our seismic profile does not show basement faults underneath both salt pillows.

A thin-skinned salt pillow evolution (Figure 10c) requires effective decoupling of the overburden from the basement. Numerous authors stated this for the northeast NGB margin (Al Hseinat & Hübscher, 2017; Hübscher et al., 2010; Kossow et al., 2000; Kossow & Krawczyk, 2002; Krauss & Mayer, 2004; Zöllner et al., 2008). Triggering of the salt flow in the Bay of Mecklenburg occurred during E-W directed extension. Major faults underneath the salt pillows are not visible. As discussed in section 5.2.1, Norian-Rhaetian to Jurassic transtensional dextral strike slip movements within the Trans-European Suture Zone affected the WFZ ~50 km northeast of the salt pillows. This correlates directly with the initiation of salt pillow growth in the Bay of Mecklenburg. The Zechstein succession in the Bay of Mecklenburg contains relatively thick Stassfurt halite units (Figures 6a and 3). This allows effective decoupling of sub-Zechstein-induced deformation within the Trans-European Suture Zone and the distribution of deformation within a relatively wide zone in the overburden (Richard et al., 1991). Therefore, a thin-skinned reactive pillow growth is a possible mechanism. During reactive growth, regional extensional stress, as evidenced in the WFZ, creates a tectonic

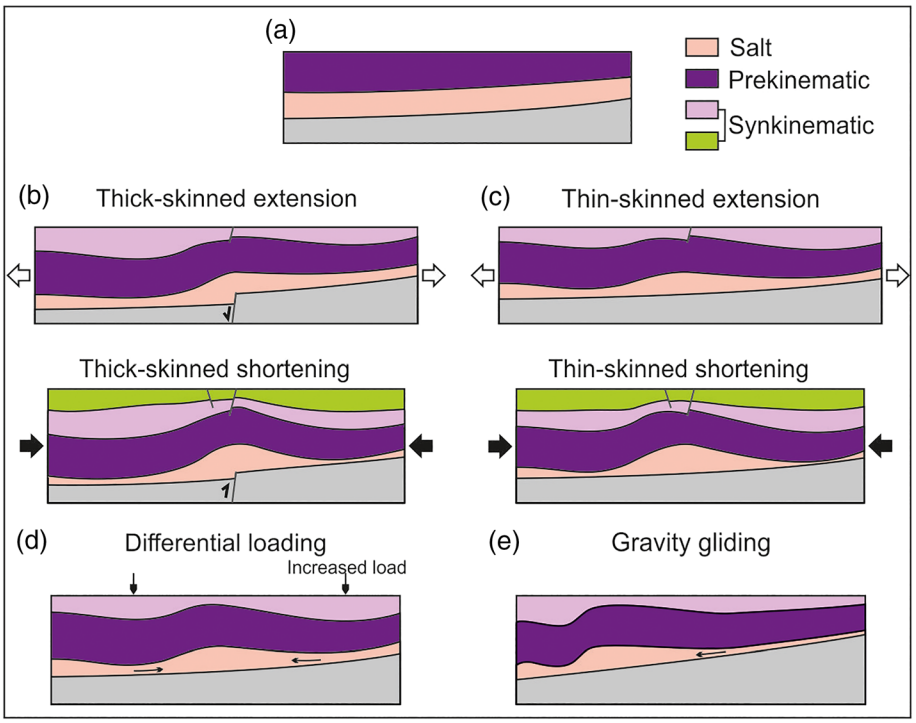

Figure 10. Sketch illustrating salt pillow growth mechanisms. (a) Initial situation with salt layer and prekinematic overburden. (b) Thick-skinned extension and subsequent thick-skinned shortening. (c) Thin-skinned extension and subsequent thin-skinned shortening. (d) Differential loading. (e) Gravity gliding. Based upon terminologies introduced by Stewart (2007), Warren (2008), Brun and Fort (2011), and Jackson and Hudec (2017).

differential load by thinning the overburden and forming grabens or half grabens. Then, pressurized salt can flow into these structurally thinned zones (as in Hudec & Jackson, 2007; Vendeville & Jackson, 1992) (Figure 10c). Initial normal crestal faults are not prominent in the Keuper successions imaged in our profile. However, the base Cretaceous unconformity directly overlies the Norian-Rhaetian deposits, which, therefore, were affected by Late Jurassic erosion that possibly removed the records of initial normal faulting. The observed salt structures never reached a diapiric stage, and thick burial by undeformed Early to Middle Triassic successions precludes an active stage. NW-SE transtensional strike slip movements within the Trans-European Suture Zone were parallel to the present-day dominant trend of salt structures within the eastern part of the NGB (Scheck-Wenderoth et al., 2008) (Figure 1). This is in agreement with a thin-skinned pillow formation.

The second phase of salt pillow growth occurred from the Coniacian-Santonian to early Cenozoic and eventually continued throughout the Cenozoic. Timing of salt pillow growth correlates with the phase of basin-wide inversion and uplift of the Grimmen High related to the onset of the Africa-Iberia-Europe convergence. Associated NE-SW directed compression induced horizontal shortening (Kley & Voigt, 2008). Due to the decoupling, thin-skinned shortening inducing salt movement is a possible growth mechanism during the second phase (as in Callot et al., 2012; Hudec & Jackson, 2007) (Figure 10c). As a result of compression, the salt's overburden may buckle, allowing the salt to flow into the low-pressure cores of overburden anticlines. Preexisting structures are especially prone to be amplified by later shortening (Hudec & Jackson, 2007; Vendeville & Nilsen, 1995). Kossow and Krawczyk (2002) mention 8.5 km of shortening of the supra-salt in the NGB, of which 70% accumulated in thrusted structures at the southern NGB margin. The remaining amount of shortening distributes over the northern basin area with decreasing deformation toward the northeastern basin margin. Uplift of the Grimmen High and inversion of the Werre Fault as a reverse fault evidence compressional forces, which possibly induced overburden buckling above the southwestern pillows. However, we do not observe any signs of thrust faulting of the salt pillow overburden. This suggests that the mobile salt effectively provided the infill of detachment folds rather than creating thrusts faults

(Stewart, 1996). Whether shortening in the Bay of Mecklenburg was sufficient to induce salt pillow growth requires further analysis. However, thin-skinned extension triggering salt pillow growth in the Late Triassic and subsequent remobilization by thin-skinned shortening in the Late Cretaceous is a possible scenario explaining salt pillow formation in the Bay of Mecklenburg (Figure 10c). The two observed phases of pillow growth correlate with regional tectonic deformation, and the thick halite units within the Zechstein sequence allow effective decoupling.

Differential loading causing downbuilding of the salt pillows is another possible mechanism for pillow growth (e.g., Jackson & Hudec, 2017) (Figure 10d). The Buntsandstein, Muschelkalk and lower Keuper show a locally relatively uniform deposition in the Bay of Mecklenburg. Accordingly, the gravitational load prior to the deposition of the Rhaetian-Norian seismic unit was rather equally distributed as evidenced by the locally uniform thickness of underlying pre-Norian sediments. This contradicts a Late Triassic triggering of salt movement by differential loading, as there is a lack of varying gravitational load between rim synclines and pillow crest. However, after an initiation by thin-skinned extension as described above, differential loading is a possible component driving ongoing salt movement during the Late Triassic and Early Jurassic due to the thicker deposits within the rim synclines. This could have resulted in increased pressure on the salt underneath the rim synclines leading to salt expulsion and pillow growth. The subsequent remobilization of salt movement in the Late Cretaceous does not fit to the concept of differential loading, as the gravitational load after the sedimentation during the Cretaceous tectonic quiescence was again rather uniform.

Gravity-driven salt movements have been intensively studied at passive margins; however, its applicability to intracontinental basins is questionable. Gravity gliding (as in Brun & Fort, 2011, 2012; Cobbold & Szatmari, 1991; Duval et al., 1992; Nalpas & Brun, 1993; Rowan et al., 2012) was discussed for some areas of the Southern Permian Basin (e.g., Warsitzka et al., 2018), and in the following, we discuss a possible effect on the salt pillow evolution at the northeastern NGB margin (Figure 10e). The second phase of observed salt flow from the Santonian to Cenozoic correlates with the phase of basinwide inversion and uplift of the basin margin including the Grimmen High. This caused increased basin margin tilt at the northeastern margin. The continuous NE migration of the local depocenter within both rim synclines suggests a SW directed downdip salt flow (Figure 7a). The base Zechstein reflector (b-PZ, Figure 7a) dips SW with ~1° in a length of ~90 km. Gravity gliding in the Kwanza Basin, offshore Angola, occurred with slope dips below 1° over distances of more than 150 km. Locally, gliding occurred at slopes of ~50 km length and angles of roughly 2.5° (Jackson & Hudec, 2005). Brun and Fort (2011) used analog models to calculate that margin tilt angles lower than 1° for wide basins (200–600 km), covered by initial sedimentary cover thickness of up to 1 km, allow dominant gliding. Shorter basins require steeper angles and less sedimentary cover. Based upon these estimations, the basin configuration of the northeastern NGB margin with ~1° slope angle over 90 km might allow gravity gliding in principle. However, the comparable short slope length and thick sedimentary overburden contradict substantial gliding and therefore might, if at all, allow only minor translation. Additionally, we need to consider some major differences in the geological setting between the two basins. The Kwanza basin is located at a passive continental margin. Sediment load concentrates updip on the slope. Gravity gliding and gravity spreading induced forces both add up in downdip direction. The NGB on the other hand is an intracontinental basin with maximum sediment load at the center. This load concentration induces counteracting, updip forces, which possibly further limit downdip salt translation. For the northeastern basin margin, salt flow by gravity gliding would be downdip in southward direction. The Bay of Mecklenburg would represent the contractional domain where shortening causes salt pillow growth, whereas the Grimmen High and WFZ correspond with the extensional domain of updip salt depletion. Zechstein thickness at the Grimmen High is not entirely reduced compared to the salt pillows in the Bay of Mecklenburg (approximately a factor of 2–3). Additionally, there is a general SW thickness increase due to the closer proximity to the basin center (e.g., Kossow et al., 2000). Hence, the overall small amount of lateral thinning indicates minor actual salt flow. The total depocenter migration in this study is less than 2 km. This also fits to an interpretation of only minor salt translation comparing to the relatively huge depocenter migrations of more than 5 km observed by Jackson and Hudec (2005) in the Kwanza basin. Their modeling results showed that a high ratio of aggradation rate to translation rate down the ramp ($\dot{A}/\dot{T}$) results in steeply dipping depocenter traces while a low $\dot{A}/\dot{T}$ ratio creates gently dipping depocenter traces. The steeply dipping depocenter traces observed in the Bay of Mecklenburg suggest a high $\dot{A}/\dot{T}$ ratio. This is either caused

by a high amount of sedimentation or minor actual salt flow down the slope. Both are consistent with our observations. A thick overburden overlies the Zechstein sequence, and actual salt flow seems minor due to considerations above. Based upon this discussion, gravity gliding might not have played a dominant role at the northeastern NGB margin. Salt flow is more likely controlled by thin-skinned extensional and compressional deformation. However, gravity gliding could have temporally contributed and caused minor downdip salt flow. We propose a scenario of gravity gliding induced slow creeping down the tilted basin slope during the Late Cretaceous to Cenozoic. This resulted in updip salt depletion at the Grimmen High and accumulation within the investigated salt pillows. Consequently, only minor updip thin-skinned extension without significant faulting occurred.

We analyzed lateral salt flow based on a NE-SW directed seismic profile. Our results provide valuable findings and mark a first step for further studies, where we strive for a comprehensive reconstruction and timing of salt movements in the whole area of the Baltic Sea sector by means of further available multichannel seismic data. This will allow addressing lateral salt movement in all directions and their influence on the structural development of the area. Depth conversion and section restoration of the seismic profile analyzed in this paper will be part of future work.

6. Summary

For the first time, we present a complete image from the base of the Zechstein to the seafloor ranging from the Bay of Mecklenburg to the northeast of Rügen Island. The seismic section images Late Permian to recent Cenozoic deposits.

The basin margin faults of the AFS and associated WFZ initiated during ENE-WSW extension in the Late Triassic. In between, subsidence in the Prerow Depression formed a marginal subbasin. The main phase of subsidence attributes to the Rhaetian-Norian until Early Jurassic times, where transtensional dextral strike slip movements within the Trans-European Suture Zone dominated.

The WFZ is reinterpreted as an inverted thin-skinned normal fault zone forming a rollover structure detached close to the base Zechstein. Antithetic normal faults are associated with the Prerow Fault Zone and suggest thin-skinned deformation related to the subsiding hanging wall of the Werre Fault. Faulting began in the Late Triassic and is associated with the formation of the Western Pomeranian Fault System.

Major plate reorganization related to the Africa-Iberia-Europe collision led to basin-scale inversion and uplift of the Grimmen High at the northeastern NGB margin. Uplift started in the Santonian-Coniacian with increased activity during the Maastrichtian-Campanian and amounts to values ranging from 460 to 570 m. This led to erosion of much of the Cretaceous succession of the Grimmen High and within the WFZ. The Werre Fault was inverted as a reverse fault causing uplift and erosion of the hanging wall.

Salt pillow growth in the Bay of Mecklenburg initiated in the Late Triassic in an extensional tectonic regime. Continuous growth until the Jurassic preserved thicker Late Triassic and Early Jurassic deposits in the rim synclines while thinning and partly erosion occurred above the pillow crests. A second phase of salt pillow growth was in the Late Cretaceous to Cenozoic correlating with the onset of basin inversion and reverse faulting in the WFZ.

We discussed salt pillow evolution in the Bay of Mecklenburg and invoked two possible driving mechanisms. In the first scenario, a thin-skinned extensional initialization in the Late Triassic and Jurassic was followed by Late Cretaceous-Cenozoic thin-skinned shortening, which led to further salt pillow growth. The second scenario discusses an effect of gravity gliding induced by basin margin tilt during the Late Cretaceous to Cenozoic. This could add to local salt flow by slow downdip creeping resulting in updip depletion, downdip salt accumulation, and pillow formation.

Acknowledgments

We would like to thank the reviewers Piotr Krzywiec and Heijn W. van Gent for their critical reading and great suggestions, which significantly improved the manuscript. Further, we are thankful to Heidrun Stück, Fabian Jähne-Klingberg, and Elisabeth Seidel for their helpful remarks on the interpretation as well as their help on improving the manuscript. We would like to thank Mark Rowan for fruitful discussions at the EGU General Assembly 2018. Data are available from the Federal Institute for Geosciences and Natural Resources (BGR) (https://www.geo-seas.eu/report/2633203). The authors thank Neptune Energy for providing additional seismic lines for stratigraphic correlation. We thank Emerson for providing licenses of their software under the Paradigm University Research Program. This project is funded by the Deutsche Forschungsgemeinschaft (DFG, German Research Foundation), Grant NO 1375/1-1. The authors declare that they have no conflict of interest.

References

Al Hseinat, M., & Hübscher, C. (2017). Late Cretaceous to recent tectonic evolution of the North German Basin and the transition zone to the Baltic Shield/southwest Baltic Sea. *Tectonophysics*, *708*, 28–55. https://doi.org/10.1016/j.tecto.2017.04.021

Al Hseinat, M., Hübscher, C., Lang, J., Lüdmann, T., Ott, I., & Polom, U. (2016). Triassic to recent tectonic evolution of a crestal collapse graben above a salt-cored anticline in the Glückstadt Graben/North German Basin. *Tectonophysics*, *680*, 50–66. https://doi.org/10.1016/j.tecto.2016.05.008

BABEL Working Group (1991). Deep seismic survey images the structure of the Tornquist Zone beneath the Southern Baltic Sea. *Geophysical Research Letters*, *18*, 1091–1094. https://doi.org/10.1029/91GL00847

BABEL Working Group (1993). Deep seismic reflection/refraction interpretation of crustal structure along BABEL Profiles A and B in the southern Baltic Sea. *Geophysical Journal International*, *122*, 325–343. https://doi.org/10.1111/j.1365-246X.1993.tb01173.x

Bachmann, G., Geluk, M., Warrington, G., Becker-Roman, A., Beutler, G., Hagdorn, H., et al. (2010). Triassic. In H. Doornenbal, & A. Stevenson (Eds.), *Petroleum geological atlas of the southern Permian Basin area* (pp. 149–173). Houten, Netherlands: European Association of Geoscientists & Engineers.

Bachmann, G. H., Voigt, T., Bayer, U., von Eynatten, H., Legler, B., & Littke, R. (2008). Depositional history and sedimentary cycles in the Central European Basin System. In R. Littke, U. Bayer, D. Gajewski, & S. Nelskamp (Eds.), *Dynamics of complex intracontinental basins, the Central European Basin System* (pp. 17–34). Berlin, Heidelberg, Germany: Springer Verlag. https://doi.org/10.1007/978-3-540-85085-4

Baldschuhn, R., Frisch, U., & Kockel, F. (2001). *The basement block pattern in Northwest Germany, scale 1:500000*. Hannover, Germany: Bundesanstalt für Geowissenschaften und Rohstoffe.

Benek, R., Kramer, W., McCann, T., Scheck, M., Negendank, J. F. W., Korich, D., et al. (1996). Permo-carboniferous magmatism of the Northeast German Basin. *Tectonophysics*, *266*(1-4), 379–404. https://doi.org/10.1016/S0040-1951(96)00199-0

Berthelsen, A. (1992). Tectonic evolution of Europe. From Precambrian to Variscan Europe. In D. Blundell (Ed.), *A continent revealed: The European Geotraverse* (pp. 153–164). Cambridge: Cambridge University Press.

Berthelsen, A. (1998). The Tornquist Zone northwest of the Carpathians: An intraplate pseudosuture. *GFF*, *120*, 223–230. https://doi.org/10.1080/11035899801202223

Best, G. (1996). Raft tectonics in Northern Germany: First results of the seismic investigations at the salt structure "Oberes Allertal". *German Journal of Geology*, *147*, 455–464.

Beutler, G., Ditrich, D., Dockter, J., Ernst, R., Etzold, A., Farrenschon, J., et al. (2005). Stratigraphie von Deutschland IV – Keuper. *Courier Forschungsinstitut Senckenberg, Germany*, *253*, 1–296.

Beutler, G., Junker, R., Niediek, S., & Rößler, D. (2012). Tektonische Diskordanzen und tektonische Zyklen im Mesozoikum Nordostdeutschlands. *Zeitschrift für Geologische Wissenschaften*, *163*, 447–468. https://doi.org/10.1127/1860-1804/2012/0163-0447

Beutler, G., & Schüler, F. (1978). Die altkimmerischen Bewegungen im Norden der DDR und ihre regionale Bedeutung. *Zeitschrift für Geologische Wissenschaften*, *6*, 403–420.

Blanc, E. J. P., Allen, M. B., Inger, S., & Hassani, H. (2003). Structural styles in the Zagros Simple Folded Zone, Iran. *Journal of the Geological Society*, *160*, 401–412. https://doi.org/10.1144/0016-764902-110

Brink, H., Franke, D., Hoffmann, N., Horst, W., & Oncken, O. (1990). Structure and evolution of the North German Basin. In R. Freeman, P. Giese, & S. Müller (Eds.), *The European geotraverse: Integrative studies*, (195–212). Strasbourg: European Science Foundation.

Brun, J.-P., & Fort, X. (2011). Salt tectonics at passive margins: Geology versus Models. *Marine and Petroleum Geology*, *28*(6), 1123–1145. https://doi.org/10.1016/j.marpetgeo.2011.03.004

Brun, J.-P., & Fort, X. (2012). Salt tectonics at passive margins: Geology versus models—Reply. *Marine and Petroleum Geology*, *37*(1), 195–208. https://doi.org/10.1016/j.marpetgeo.2012.04.008

Callot, J.-P., Trocmé, V., Letouzey, J., Albouy, E., Jahani, S., & Sherkati, S. (2012). Pre-existing salt structures and the folding of the Zagros Mountains. *Geological Society, London, Special Publications*, *363*(1), 545–561. https://doi.org/10.1144/sp363.27

Cobbold, P. R., & Szatmari, P. (1991). Radial gravitational gliding on passive margins. *Tectonophysics*, *188*(3-4), 249–289. https://doi.org/10.1016/0040-1951(91)90459-6

Coleman, A. J., Jackson, C. A. L., & Duffy, O. B. (2017). Balancing sub-and supra-salt strain in salt-influenced rifts: Implications for extension estimates. *Journal of Structural Geology*, *116*, 1–11. https://doi.org/10.1016/j.jsg.2018.08.006

Coward, M. P. (1983). Thrust tectonics, thin skinned or thick skinned, and the continuation of thrusts to deep in the crust. *Journal of Structural Geology*, *5*(2), 113–123. https://doi.org/10.1016/0191-8141(83)90037-8

Davis, D. M., & Engelder, T. (1985). The role of salt in fold-and-thrust belts. *Tectonophysics*, *119*(1–4), 67–88. https://doi.org/10.1016/0040-1951(85)90033-2

DEKORP-BASIN Research Group (1999). Deep crustal structure of the Northeast German basin: New DEKORP-BASIN'96 deep-profiling results. *Geology*, *27*(1), 55–58. https://doi.org/10.1130/0091-7613(1999)027<0055:DCSOTN>2.3.CO;2

Deutschmann, A., Meschede, M., & Obst, K. (2018). Fault system evolution in the Baltic Sea area west of Rügen, NE Germany. In B. Kilhams, P. Kukla, S. Mazur, T. McKie, H. Munlieff, & K. van Ojik (Eds.), *Mesozoic resource potential in the southern Permian Basin, special publications* (Vol. 469, pp. 83–98). London: The Geological Society. https://doi.org/10.1144/sp469.24

Duval, B., Cramez, C., & Jackson, M. P. A. (1992). Raft tectonics in the Kwanza Basin, Angola. *Marine and Petroleum Geology*, *9*(4), 389–404. https://doi.org/10.1016/0264-8172(92)90050-O

Erlström, M., Thomas, S., Deeks, N., & Sivhed, U. (1997). Structure and tectonic evolution of the Tornquist Zone and adjacent sedimentary basins in Scania and the southern Baltic Sea area. *Tectonophysics*, *271*(3-4), 191–215. https://doi.org/10.1016/S0040-1951(96)00247-8

EUGENO-S Working Group (1988). Crustal structure and tectonic evolution of the transition between the Baltic Shield and the North German Caledonides. *Tectonophysics*, *150*(3), 253–348. https://doi.org/10.1016/0040-1951(88)90073-X

Frisch, U., & Kockel, F. (1999). Quantification of Early Cimmerian movements in NW-Germany. *Zentralblatt für Geologie und Paläontologie, Teil*, *1*(1–2), 571–600.

Gast, R., Pasternak, M., Piske, J., & Rasch, H.-J. (1998). Rotliegend in northeastern Germany: Regional overview, stratigraphy facies and diagenesis. *Geologisches Jahrbuch der BGR, A*, *149*, 59–79.

Geißler, M., Breitkreuz, C., & Kiersnowski, H. (2008). Late Paleozoic volcanism in the central part of the Southern Permian Basin (NE Germany, W Poland): Facies distribution and volcano-topographic hiati. *International Journal of Earth Sciences*, *97*(5), 973–989. https://doi.org/10.1007/s00531-007-0288-6

Graversen, O. (2006). The Jurassic-Cretaceous North Sea rift dome and associated basin evolution. *AAPG Search and Discovery*, #30040.

Guterch, A., Wybraniec, S., Grad, M., Chadwick, A., Krawczyk, C. M., Ziegler, P., et al. (2010). Crustal structure and structural framework. In H. Doornenbal, & A. Stevenson (Eds.), *Petroleum geological atlas of the southern Permian Basin area* (pp. 11–23). Houten, Netherlands: European Association of Geoscientists & Engineers.

Hansen, M., Lykke-Andersen, H., Dehghani, A., Gajewski, D., Hübscher, C., Olesen, M., & et al. (2005). The Mesozoic-Cenozoic structural framework of the Bay of Kiel area, western Baltic Sea. *International Journal of Earth Sciences*, *94*(5-6), 1070–1082. https://doi.org/10.1007/s00531-005-0001-6

Hansen, M., Scheck-Wenderoth, M., Hübscher, C., Lykke-Andersen, H., Dehghani, A., Hell, B., & Gajewski, D. (2007). Basin evolution of the northern part of the Northeast German Basin—Insights from a 3D structural model. *Tectonophysics*, *437*(1-4), 1–16. https://doi.org/10.1016/j.tecto.2007.01.010

Hoth, K., Rusbült, J., Zagora, K., Beer, H., & Hartmann, O. (1993). Die tiefen Bohrungen im Zentralabschnitt der Mitteleuropäischen Senke—Dokumentation für den Zeitabschnitt 1962–1990. *Verlag der Gesellschaft für Geologische Wissenschaften*, *2*(7), 1–145.

Hübscher, C., Ahlrichs, N., Allum, G., Behrens, T., Bülow, J., Krawczyk, C., et al. (2016). *MSM52 BalTec Fahrtbericht*. Hamburg, Germany: University of Hamburg. https://doi.org/10.1594/PANGAEA.890870

Hübscher, C., Hansen, M., Trinanes, S., Lykke-Andersen, H., & Gajewski, D. (2010). Structure and evolution of the Northeastern German Basin and its transition onto the Baltic Shield. *Marine and Petroleum Geology*, *27*(4), 923–938. https://doi.org/10.1016/j.marpetgeo.2009.10.017

Hübscher, C., Lykke-Andersen, H., Bak Hansen, H., & Reicherter, K. (2004). Investigating the structural evolution of the Western Baltic. *Earth and Space News*, *85*(12), 115–116.

Hudec, M. R., & Jackson, M. P. A. (2007). Terra infirma: Understanding salt tectonics. *Earth-Science Reviews*, *82*(1-2), 1–28. https://doi.org/10.1016/j.earscirev.2007.01.001

Jackson, M. P. A., & Hudec, M. R. (2005). Stratigraphic record of translation down ramps in a passive-margin salt detachment. *Journal of Structural Geology*, *27*, 889–911. https://doi.org/10.1016/j.jsg.2005.01.010

Jackson, M. P. A., & Hudec, M. R. (2017). *Salt tectonics—Principles and practice*. Cambridge, United Kingdom: Cambridge University Press.

Jackson, M. P. A., Vendeville, B. C., & Schultz-Ela, D. D. (1994). Structural dynamics of salt systems. *Annual Review of Earth and Planetary Sciences*, *22*(1), 93–117. https://doi.org/10.1146/annurev.ea.22.050194.000521

Jaritz, W. (1973). Zur Entstehung der Salzstrukturen Nordwestdeutschlands. *Geologisches Jahrbuch, A*, *10*, 1–77.

Jaritz, W. (1987). The origin and development of salt structures in Northwest Germany. In I. O'Brien, & J. Lerche (Eds.), *Dynamical geology of salt and related structures* (pp. 479–493). Cambridge: Academic Press.

Kaiser, R. (2001). *Fazies und Sequenzstratigraphie: Das Staßfurtkarbonat (Ca2) am nördlichen Beckenrand des südlichen Zechsteinbeckens (NE-Deutschland), (Doctoral dissertation)*. Cologne, Germany: University of Cologne.

Kammann, J., Hübscher, C., Boldreel, L. O., & Nielsen, L. (2016). High-resolution shear-wave seismics across the Carlsberg Fault zone south of Copenhagen—Implications for linking Mesozoic and late Pleistocene structures. *Tectonophysics*, *682*, 56–64. https://doi.org/10.1016/j.tecto.2016.05.043

Katzung, P. D. G. (2004). *Geologie von Mecklenburg-Vorpommern (Vol.1)*. Stuttgart, Germany: E. Schweizerbart'sche Verlagsbuchhandlung.

Kley, J. (2018). Timing and spatial patterns of Cretaceous and Cenozoic inversion in the Southern Permian Basin. In Kilhams, B., Kukla, P. A., Mazur, S., McKie, T., Mijnlieff, H. F., van Ojik, K. (Eds.), *Mesozoic resource potential in the southern Permian Basin*, London: The Geological Society.*Special Publications*, 469, 19–31, https://doi.org/10.1144/sp469.12

Kley, J., & Voigt, T. (2008). Late Cretaceous intraplate thrusting in central Europe: Effect of Africa-Iberia-Europe convergence, not Alpine collision. *Geology*, *36*, 839–842. https://doi.org/10.1130/g24930a.1

Kockel, F. (1999). Die Bildung von Salzstrukturen in Norddeutschland—Neue Einsichten, offene Fragen. *Mitteilungen der Deutschen Geophysikalischen Gesellschaft*, *3*, 38–47.

Kockel, F. (2002). Rifting processes in NW-Germany and the German North Sea Sector. *Netherlands Journal of Geosciences*, *81*(2), 149–158. https://doi.org/10.1017/S0016774600022381

Kossow, D., & Krawczyk, C. M. (2002). Structure and quantification of processes controlling the evolution of the inverted NE-German Basin. *Marine and Petroleum Geology*, *19*(5), 601–618. https://doi.org/10.1016/S0264-8172(02)00032-6

Kossow, D., Krawczyk, C. M., McCann, T., Strecker, M., & Negendank, J. F. W. (2000). Style and evolution of salt pillows and related structures of the northern part of the Northeast German Basin. *International Journal of Earth Sciences*, *89*(3), 652–664. https://doi.org/10.1007/s005310000116

Krauss, M., & Mayer, P. (2004). The Vorpommern fault system and its regional structural relationship to the Trans-European Fault Zone. *Zeitschrift für Geologische Wissenschaften*, *32*(2–4), 227–246.

Krawczyk, C., Eilts, F., Lassen, A., & Thybo, H. (2002). Seismic evidence of Caledonian deformed crust and uppermost mantle structures in the northern part of the Trans-European Suture Zone, SW Baltic Sea. *Tectonophysics*, *360*(1-4), 215–244. https://doi.org/10.1016/S0040-1951(02)00355-4

Krawczyk, C., Rabbel, W., Willert, S., Hese, F., Götze, H.-J., Gajewski, D., & the SPP-Geophysics Group (2008a). Crustal structures and properties in the Central European Basin system from geophysical evidence. In R. Littke, U. Bayer, D. Gajewski, & S. Nelskamp (Eds.), *Dynamics of Complex Intracontinental Basins* (pp. 67–95). Berlin, Heidelberg, Germany: Springer-Verlag. https://doi.org/10.1007/978-3-540-85085-4

Krawczyk, C. M., McCann, T., Cocks, L. R. M., England, R., McBride, J., & Wybraniec, S. (2008b). Caledonian Tectonics. In T. McCann (Ed.), *The geology of Central Europe* (Vol. 1, pp. 2–115). London: The Geological Society.

Krzywiec, P. (2012). Mesozoic and Cenozoic evolution of salt structures within the Polish basin: An overview. In G. I. Alsop, S. G. Archer, A. J. Hartley, N. T. Grant, & R. Hodgkinson (Eds.), *Salt Tectonics, Sediments and Prospectivity, Special Publications* (Vol. 363, pp. 381–394). London: The Geological Society. https://doi.org/10.1144/SP363.17

Krzywiec, P., Kiersnowski, H., & Peryt, T. (2019). Fault-controlled Permian sedimentation in the central Polish Basin (Bydgoszcz-Szubin area)—Insights from well and seismic data. *Zeitschrift der Deutschen Gesellschaft für Geowissenschaften (German Journal of Geology)*, *170*(3–4), 255–272. https://doi.org/10.1127/zdgg/2019/0198

Krzywiec, P., Peryt, T. M., Kiersnowski, H., Pomianowski, P., Czapowski, G., & Kwolek, K. (2017). Permo-Triassic evaporites of the Polish Basin and their bearing on the tectonic evolution and hydrocarbon system, an overview. In J. Soto, J. Flinch, & G. Tari (Eds.), *Permo-Triassic salt provinces of Europe, North Africa and the Central Atlantic: Tectonics and hydrocarbon potential* (pp. 243–261). Amsterdam, Netherlands: Elsevier. https://doi.org/10.1016/B978-0-12-809417-4.00012-4

Kukla, P. A., Urai, J. L., & Mohr, M. (2008). Dynamics of salt structures. In R. Littke, U. Bayer, D. Gajewski, & S. Nelskamp (Eds.), *Dynamics of complex intracontinental basins, the Central European Basin System* (pp. 249–276). Berlin, Heidelberg, Germany: Springer-Verlag. https://doi.org/10.1007/978-3-540-85085-4

Maystrenko, Y., Bayer, U., Brink, H.-J., & Littke, R. (2008). The Central European Basin System - an Overview. In R. Littke, U. Bayer, D. Gajewski, & S. Nelskamp (Eds.), *Dynamics of complex intracontinental basins, the Central European Basin System* (pp. 17–34). Berlin, Heidelberg, Germany: Springer Verlag. https://doi.org/10.1007/978-3-540-85085-4

Maystrenko, Y., Bayer, U., & Scheck-Wenderoth, M. (2005). Structure and evolution of the Glückstadt Graben due to salt movement. *International Journal of Earth Sciences*, *94*, 799–814. https://doi.org/10.1007/s00531-005-0003-4

Maystrenko, Y., Bayer, U., & Scheck-Wenderoth, M. (2006). 3D reconstruction of salt movements within the deepest post-Permian structure of the Central European Basin System—The Glueckstadt Graben. *Netherlands Journal of Geosciences/Mijnbouw*, *85*(3), 181–196. https://doi.org/10.1017/S0016774600021466

Maystrenko, Y., Bayer, U., & Scheck-Wenderoth, M. (2012). Salt as a 3D element in structural modelling—Example from the Central European Basin System. *Tectonophysics*, *591*, 62–82. https://doi.org/10.1016/j.tecto.2012.06.030

Mazur, S., Aleksandrowski, P., Gagala, L., Krzywiec, P., Zaba, J., Gaidzik, K., & Sikora, R. (2020). Late Paleozoic strike-slip tectonics versus oroclinal bending at the SW outskirts of Baltica: Case of the Variscan belt's eastern end in Poland. *International Journal of Earth Sciences*, *109*(4), 1133–1160. https://doi.org/10.1007/s00531-019-01814-7

Mazur, S., Mikolajczak, M., Krzywiec, P., Malinowski, M., Buffenmyer, V., & Lewandowski, M. (2015). Ist he Teisseyre-Tornquist Zone an ancient plate boundary of Baltica? *Tectonics*, *34*, 2465–2477. https://doi.org/10.1002/2015TC003934

Meinhold, R., & Reinhardt, H. G. (1967). Halokinese im Nordostdeutschen Tiefland. *Berichte der Deutschen Gesellschaft für Geologische Wissenschaften*, *12*, 329–353.

Menning, M. (2016). The stratigraphic table of Germany 2016 (STD 2016). *German Journal of Geology*, *169*, 105–128.

Mohr, M., Kukla, P. A., Urai, J. L., & Bresser, G. (2005). Multiphase salt tectonic evolution in NW Germany: Seismic interpretation and retro-deformation. *International Journal of Earth Sciences*, *94*, 917–940. https://doi.org/10.1007/s00531-005-0039-5

Nalpas, T., & Brun, J. P. (1993). Salt flow and diapirism related to extension at crustal scale. *Tectonophysics*, *228*, 349–362. https://doi.org/10.1016/0040-1951(93)90348-N

Nielsen, L. H., & Japsen, P. (1991). Deep wells in Denmark—1935–1990. *Danmarks Geologiske Undersøgelse Serie A*, *31*, 177.

Noack, V., Schnabel, M., Damm, V., & Hübscher, C. (2018). *Velocity model building for depth conversion and interpretation of multi-channel seismic data in the Mecklenburg Bay of the southern Baltic Sea*. Celle, Germany: Paper presented at DGMK/ÖGEW-Frühjahrstagung.

Nöldeke, W., & Schwab, G. (1976). Zur tektonischen Entwicklung des Tafeldeckgebirges der Norddeutsch-Polnischen Senke unter besonderer Berücksichtigung des Nordteils der DDR. *Zeitschrift für Angewandte Geologie*, *23*, 369–379.

Pharaoh, T. (1999). Palaeozoic terranes and their lithospheric boundaries within the Trans-European Suture Zone (TESZ): A review. *Tectonophysics*, *314*, 17–41. https://doi.org/10.1016/S0040-1951(99)00235-8

Pharaoh, T., Dusar, M., Geluk, M., Kockel, F., Krawczyk, C., Krzywiec, P., et al. (2010). Tectonic evolution. In H. Doornenbal, & A. Stevenson (Eds.), *Petroleum geological atlas of the southern Permian Basin area* (pp. 25–57). Houten, Netherlands: European Association of Geoscientists & Engineers.

Pichel, L., Huuse, M., Redfern, J., & Finch, E. (2019). The influence of base-salt relief, rift topography and regional events on salt tectonics offshore Morocco. *Marine and Petroleum Geology*, *103*, 87–1113. https://doi.org/10.1016/j.marpetgeo.2019.02.007

Prather, B. E., Booth, J. R., Steffens, G. S., & Craig, P. A. (1998). Classification, lithologic calibration and stratigraphic succession of seismic facies of intraslope basins, deep-water Gulf of Mexico. *AAPG Bulletin*, *52*, 701–728. https://doi.org/10.1306/1D9BC5D9-172D-11D7-8645000102C1865D

Reiche, S., Hübscher, C., & Beitz, M. (2014). Fault-controlled evaporate deformation in the Levant Basin, Eastern Mediterranean. *Marine Geology*, *354*, 53–68. https://doi.org/10.1016/j.margeo.2014.05.002

Reinhardt, H.-G. (1993). Structure of Northeast Germany: Regional depth and thickness maps of Permian to tertiary intervals compiled from seismic reflection data. In A. M. Spencer (Ed.), *Generation, accumulation and production of Europe's hydrocarbons III* (pp. 155–165). Berlin, Heidelberg, Germany: Springer, Special Publication of the European Association of Petroleum Geoscientists.

Reinhold, K., Krull, P., & Kockel, F. (2008). *Salzstrukturen Norddeutschlands, scale 1:500000*. Berlin, Hannover, Germany: Bundesanstalt für Geowissenschaften und Rohstoffe.

Rempel, H. (1992). Erdölgeologische Bewertung der Arbeiten der Gemeinsamen Organisation Petrobaltic im deutschen Schelfbereich. *Geologisches Jahrbuch*, *D99*, 3–32.

Richard, P., Mocquet, B., & Cobbold, P. R. (1991). Experiments on simultaneous faulting and folding above a basement wrench fault. *Tectonophysics*, *188*, 133–141. https://doi.org/10.1016/0040-1951(91)90319-N

Rowan, M., Peel, F., Vendeville, B., & Gaullier, V. (2004). Gravity-driven fold belts on passive Margins. *American Association of Petroleum Geologists Memoir*, *82*, 157–182.

Rowan, M., Peel, F., Vendeville, B., & Gaullier, V. (2012). Salt tectonics at passive margins: Geology versus models—Discussion. *Marine and Petroleum Geology*, *37*, 184–194. https://doi.org/10.1016/j.marpetgeo.2012.04.007

Rühberg, N. (1976). Probleme der Zechsteinsalzbewegung. *Zeitschrift für Angewandte Geologie*, *22*, 413–420.

Sangree, J. B., & Widmier, J. M. (1979). Interpretation of depositional facies from seismic data. *Geophysics*, *44*(2), 131–160. https://doi.org/10.1190/1.1440957

Scheck, M., Barrio-Alvers, L., Bayer, U., & Götze, H.-J. (1999). Density structure of the Northeast German Basin: 3D modelling along the DEKORP Line BASIN96. *Physics and Chemistry of the Earth*, *24*(3), 221–230. https://doi.org/10.1016/S1464-1895(99)00022-8

Scheck, M., & Bayer, U. (1999). Evolution of the Northeast German Basin—Inferences from a 3D structural model and subsidence analysis. *Tectonophysics*, *313*(1-2), 145–169. https://doi.org/10.1016/S0040-1951(99)00194-8

Scheck, M., Bayer, U., & Lewerenz, B. (2003). Salt movements in the North German Basin and its relation to major post-Permian tectonic phases—Results from 3D structural modelling, backstripping and reflection seismic data. *Tectonophysics*, *361*(3-4), 277–299. https://doi.org/10.1016/s0040-1951(02)00650-9

Scheck-Wenderoth, M., Maystrenko, Y., Hübscher, C., Hansen, M., & Mazur, S. (2008). Dynamics of salt basins. In R. Littke, U. Bayer, D. Gajewski, & S. Nelskamp (Eds.), *Dynamics of complex intracontinental basins, the Central European Basin System* (pp. 17–34). Berlin, Heidelberg, Germany: Springer Verlag. https://doi.org/10.1007/978-3-540-85085-4

Schlüter, D., Jürgens, D., Best, G., Binot, F., & Stamme, H. (1997). *Analyse geologischer und geophysikalischer Daten aus der südlichen Ostsee—Strukturatlas südliche Ostsee (SASO)*. Berlin, Hannover, Germany: Bundenanstalt für Geowissenschaften und Rohstoffe.

Schröder, B. (1982). Entwicklung des Sedimentbeckens und Stratigraphie der klassischen Germanischen Trias. *Geologische Rundschau*, *71*(3), 783–794. https://doi.org/10.1007/BF01821103

Seidel, E., Meschede, M., & Obst, K. (2018). The Wiek Fault System east of Rügen Island: Origin, tectonic phases and its relationship to the Trans-European Suture Zone. In B. Kilhams, P. Kukla, S. Mazur, T. McKie, H. Munlieff, & K. van Ojik (Eds.), *Mesozoic resource potential in the southern Permian Basin* (Vol. 469, pp. 59–82). London: The Geological Society. https://doi.org/10.1144/sp469.10

Sørensen, K. (1986). Rim syncline volume estimation and salt diapirism. *Nature*, *319*, 23–27. https://doi.org/10.1038/319023a0

Steward, S. A., & Coward, M. P. (1996). Genetic interpretation and mapping of salt structures. *First Break*, *14*(4), 135–141. https://doi.org/10.3997/1365-2397.1996009

Stewart, S. A. (1996). Influence of detachment layer thickness on style of thin-skinned shortening. *Journal of Structural Geology*, *18*(10), 1271–1274. https://doi.org/10.1016/S0191-8141(96)00052-1

Stewart, S. A. (2007). Salt tectonics in the North Sea Basin: A structural style template for seismic interpreters. In A. C. Ries, R. W. H. Butler, & R. H. Graham (Eds.), *Deformation of the Continental Crust: The legacy of Mike Coward*. Geological Society, (Vol. 272, pp. 361–396). London: Special Publications. https://doi.org/10.1144/GSL.SP.2007.272.01.19

Strohmenger, C., Voigt, E., & Zimdars, J. (1996). Sequence stratigraphy and cyclic development of Basal Zechstein carbonate-evaporite deposits with emphasis on Zechstein 2 off-platform carbonates (Upper Permian, Northeast Germany). *Sedimentary Geology*, *102*, 33–54. https://doi.org/10.1016/0037-0738(95)00058-5

Strozyk, F., van Gent, H., Urai, J. L., & Kukla, P. A. (2012). 3D seismic study of complex intra-salt deformation: An example from the Upper Permian Zechstein 3 stringer in the western Dutch offshore. *Geological Society, London, Special Publications*, *363*, 489–501. https://doi.org/10.1144/SP363.23

Thieme, B., & Rockenbauch, K. (2001). Triassic rift-raft tectonics in the German Southern North Sea. *Erdöl, Erdgas, Kohle*, *117*, 568–573.

Trusheim, F. (1960). Mechanism of salt migration in northern Germany. *AAPG Bulletin*, *44*(9), 1519–1540. https://doi.org/10.1306/0BDA61CA-16BD-11D7-8645000102C1865D

Tucker, M. E. (1991). Sequence stratigraphy of carbonate-evaporite basins; models and application to the Upper Permian (Zechstein) of Northeast England and adjoining North Sea. *Journal of the Geological Society of London*, *148*, 1019–1036. https://doi.org/10.1144/gsjgs.148.6.1019

Underhill, J. R. (1998). Jurassic. In K. W. Glennie (Ed.), *Petroleum geology of the North Sea: Basic concepts and recent advances* (Vol. 4, pp. 245–293). Malden, U.S.A: Blackwell Science.

Underhill, J. R., & Partington, M. A. (1993). Jurassic thermal doming and deflation in the North Sea: Implications of the sequence stratigraphic evidence. *Geological Society, London, Petroleum Geology Conference series*, *4*, 337–345. https://doi.org/10.1144/0040337

Van Gent, H., Urai, J. L., & Keijzer, M. (2010). The internal geometry of salt structures—A first look using 3D seismic data from the Zechstein of the Netherlands. *Structural Geology*, 1–20. https://doi.org/10.1016/j.tecto.2008.09.038

Van Wees, J.-D., Stephenson, R., Ziegler, P. A., Bayer, U., McCann, T., & Dadlez, et al. (2000). On the origin of the Southern Permian Basin, Central Europe. *Marine and Petroleum Geology*, *17*, 43–59. https://doi.org/10.1016/S0264-8172(99)00052-5

Vejbaek, O. V. (1997). Dybe strukturer i danske sedimentære bassiner. *Geologisk Tidsskrift*, *4*, 1–31.

Vejbaek, O. V., Andersen, C., Dusar, M., Herngreen, W., Krabbe, H., Leszczynski, K., et al. (2010). Cretaceous. In H. Doornenbal, & A. Stevenson (Eds.), *Petroleum geological atlas of the southern Permian Basin Area* (pp. 25–57). Houten, Netherlands: European Association of Geoscientists & Engineers.

Vejbaek, O. V., & Britze, P. (1994). Top pre-Zechstein, Geological Map of Denmark. In *In Danmarks Geologiske Undersøgelse Map series 45, (scale 1:750000*, 45, 1–9). Copenhagen, Denmark: Geological Survey of Denmark.

Vendeville, B. C., & Jackson, M. P. A. (1992). The rise of diapirs during thin-skinned extension. *Marine and Petroleum Geology*, *9*(4), 331–354. https://doi.org/10.1016/0264-8172(92)90047-I

Vendeville, B. C., & Nilsen, K. T. (1995). Episodic growth of salt diapirs driven by horizontal shortening. In C. J. Travis, H. Harrison, M. R. Hudec, B. C. Vendeville, F. J. Peel, & B. F. Perkins (Eds.), *Salt, sediment and hydrocarbons*, 16th, *16th Annual Research Conference Program and Extended Abstracts*, (285–295). Houston, U.S.A: Society of Economic Paleontologists and Mineralogists.

Verschuur, D. J. (2006). *Seismic multiple removal techniques—Past, present and future*. Houten, Netherlands: EAGE Publications.

Warren, J. (2008). Salt as sediment in the Central European Basin System as seen from a deep time perspective. In R. Littke, U. Bayer, D. Gajewski, & S. Nelskamp (Eds.), *Dynamics of complex intracontinental basins, the Central European Basin System* (pp. 249–276). Berlin, Heidelberg, Germany: Springer-Verlag. https://doi.org/10.1007/978-3-540-85085-4

Warsitzka, M., Jähne-Klingberg, F., Kley, J., & Kukowski, N. (2018). The timing of salt structure growth in the Southern Permian Basin (Central Europe) and implications for basin dynamics. *Basin Research*, 1–24. https://doi.org/10.1111/bre.12323

Withjack, M. O., & Callaway, S. (2000). Active normal faulting beneath a salt layer: An experimental study of deformation patterns in the cover sequence. *AAPG Bulletin*, *84*(5), 627–651. https://doi.org/10.1306/C9EBCE73-1735-11D7-8645000102C1865D

Zagora, I., & Zagora, K. (1997). An Upper Permian (Ca1) Reef in the German part of the Baltic Sea. *Freiberger Forschungshefte C*, *466*(4), 19–31.

Ziegler, P. (1990). Tectonic and paleogeographic development of the North Sea rift system. In D. Blundell, & A. D. Gibbs (Eds.), *Tectonic Evolution of the North Sea Rifts* (pp. 1–36). New York: Oxford University Press.

Zöllner, H., Reicherter, K., & Schikowsky, P. (2008). High-resolution seismic analysis of the coastal Mecklenburg Bay (North German Basin): the pre-Alpine evolution. *International Journal of Earth Sciences*, *97*, 1013–1027. https://doi.org/10.1007/s00531-007-0277-9